

# Schedule Optimization for a Heterogeneous Earth Observation Constellation

**Florian Thomas Strasser**

Thesis for the attainment of the academic degree

**Master of Science Aerospace (M.Sc. Aerospace)**

at the TUM School of Engineering and Design of the Technical University of Munich.

**Examiner:**

Prof. Dr. Phil. Alessandro Golkar

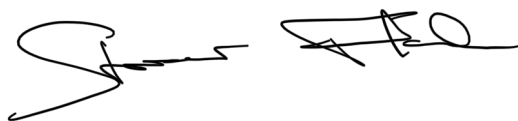
**Supervisor:**

M.Sc. Vincenzo Messina

**Submitted:**

Munich, 01.08.2023

I hereby declare that this thesis is entirely the result of my own work except where otherwise indicated. I have only used the resources given in the list of references.

A handwritten signature in black ink, consisting of a large, stylized 'S' followed by a horizontal line and a series of loops and flourishes.

Florian Thomas Strasser

Munich, 01.08.2023

# Abstract

Spacecraft operations require finding the right compromise between utilizing and preserving their available resources in the pursuit of contributing as efficiently as possible to their declared mission goals. To achieve this balance, key resources such as data storage and downlink, power, thermal range, payload, and stakeholder interests need to be carefully managed. Managing the approach to the scheduling of operations for a single spacecraft has shown to exceed the capacity of human operators. Moreover, the challenges increase significantly when multiple assets are involved in a constellation, leading to new use cases and requirements.

The goal of this thesis is to define and implement an optimization approach to the scheduling of a heterogeneous Earth observation satellite constellation accounting for both mission success criteria as well as cost-effectiveness of the operations, while also taking into account all other relevant resource constraints. This approach was developed and implemented in preparation for the integration of the FOREST-2 satellite mission developed by OroraTech into an expanding constellation of satellites used for detecting wildfires. The algorithmic approach is based on the strategy used during the operational phase of the FOREST-1 mission, which served as a predecessor to FOREST-2.

Special consideration was given to how changes in the number of satellites and orbital planes, together with the manner in which they are placed on them, impact overall constellation performance, especially with regard to measures such as continuous coverage and maximum revisit times. However, this concept is in principle transferable to the operations of any Low-Earth Orbit Earth observation satellite constellation. The state of the art of commonly used approaches for the scheduling of constellations of Earth observation satellites is presented and evaluated with respect to their suitability for the task at hand, and compared to the proposed approach. The model description and implementation into the scheduling workflow are introduced and the scheduling results for a selection of constellation design scenarios are presented in order to assess and validate the optimization efforts of this work. These test cases range from two single satellites to one, two, and four planes with eight satellites each, to the case of eighteen satellites on as many orbital planes. The average resource allocation has been proven to show a full allocation of the available data budget for each case apart from the two-satellite example. Further, the data budget could be identified as the limiting factor, with average power budget allocations in the range of 20-35%. It has been demonstrated that the fulfillment rate of imaging orders is significantly improved by first sizing each plane for continuous ground coverage, and then adding more orbital planes with the same minimum number of satellites in each, compared to randomly assembling a constellation of individual satellites.

# Zusammenfassung

Für den Betrieb von Raumfahrzeugen muss der richtige Kompromiss zwischen der Nutzung und der Erhaltung ihrer verfügbaren Ressourcen gefunden werden, um so effizient wie möglich zur Erreichung ihrer erklärten Missionsziele beizutragen. Um dieses Gleichgewicht zu erreichen, müssen Schlüsselressourcen wie Datenspeicher und Downlink, elektrische Leistung, thermische Rahmenbedingungen, Nutzlast und die Interessen aller Beteiligten sorgfältig gesteuert werden. Es hat sich gezeigt, dass das Management des Betriebskonzepts bereits für ein einzelnes Raumfahrzeug die Kapazitäten eines menschlichen Betreibers übersteigt. Außerdem wachsen die Herausforderungen erheblich, sobald mehrere Satelliten als eine Konstellation behandelt werden, was zu neuen Anwendungsfällen und Anforderungen führt.

Das Ziel dieser Arbeit ist die Definition und Implementierung eines Optimierungsansatzes für die Betriebsplanung einer heterogenen Erdbeobachtungssatellitenkonstellation, der sowohl Missionserfolgskriterien als auch die Kosteneffizienz des Betriebs berücksichtigt und dabei auch alle anderen relevanten Ressourcenbeschränkungen miteinbezieht. Dieser Ansatz wurde in Vorbereitung auf die Integration der von OroraTech entwickelten Satellitenmission FOREST-2 in eine wachsende Konstellation von Satelliten zur Früherkennung von Waldbränden entwickelt und umgesetzt. Der Algorithmus-orientierte Ansatz basiert auf der Strategie, die während der operationellen Phase der FOREST-1 Mission verwendet wurde, die als Vorläufer der FOREST-2 Mission diente.

Besonderes Augenmerk wurde darauf gelegt, wie sich Änderungen in der Anzahl der Satelliten, in den Bahnebenen und in der Art und Weise ihrer Positionierung auf die Gesamtleistung der Konstellation auswirken, insbesondere im Hinblick auf Parameter wie die kontinuierliche Abdeckung und die maximalen Zeitabstände zwischen zwei Überflügen. Im Prinzip soll sich dieses Konzept auf den Betrieb jeder beliebigen Konstellation von Erdbeobachtungssatelliten in niedrigen Erdumlaufbahnen übertragen lassen. Der aktuelle Stand gängiger Ansätze für die Planung von Konstellationen von Erdbeobachtungssatelliten wird vorgestellt, im Hinblick auf ihre Eignung für die vorliegende Themenstellung bewertet und mit dem vorgeschlagenen Ansatz verglichen. Darüber hinaus werden die Modellbeschreibung und die Implementierung in den Planungsablauf vorgestellt und die Ergebnisse für eine Auswahl von Konstellationsszenarien präsentiert, um die Bemühungen im Hinblick auf Optimierung dieser Arbeit zu bewerten und zu validieren. Diese Testabläufe reichen von zwei einzelnen Satelliten über eine, zwei und vier Bahnebenen mit jeweils acht Satelliten bis hin zum Fall von achtzehn Satelliten auf ebenso vielen Bahnebenen. Es hat sich gezeigt, dass die durchschnittliche Ressourcenzuweisung das verfügbare Datenbudget in jedem Fall vollständig ausschöpft, mit Ausnahme des Beispiels mit zwei Satelliten. Darüber hinaus konnte das Datenbudget als begrenzender Faktor identifiziert werden, wohingegen die durchschnittliche Zuweisung das Energiebudgets im Bereich von 20-35% lag. Es konnte festgestellt werden, dass sich die Erfüllungsrate von Aufträgen für Bildaufnahmen erheblich verbessert, wenn zunächst jede Ebene für eine kontinuierliche Bodenabdeckung dimensioniert wird und dann weitere Bahnebenen mit der gleichen Mindestanzahl von Satelliten hinzugefügt werden, verglichen mit einer zufälligen Zusammenstellung einer Konstellation aus einzelnen Satelliten.

## Acknowledgements

First and foremost, I want to express my deepest gratitude to my advisors at the Chair of Pico and Nanosatellites, and Satellite Constellations, Vincenzo Messina and Prof. Alessandro Golkar, who supervised my work and offered their support and constructive criticism throughout the process of this thesis.

Further, I want to thank my colleagues and supervisors at OroraTech for their mentoring, especially Valentin Dornauer, Till Assmann and Florian Patzwahl for providing me this opportunity to work on OroraTech's mission of empowering better decisions for climate resilience with continuous thermal data from space for a sustainable Earth.

Lastly, I would like to thank everybody else who supported me over the course of this thesis, you know who you are.

# Contents

<b>Abstract</b>	<b>iii</b>
<b>Zusammenfassung</b>	<b>iv</b>
<b>Acknowledgements</b>	<b>v</b>
<b>List of Figures</b>	<b>ix</b>
<b>List of Tables</b>	<b>x</b>
<b>Acronyms</b>	<b>xi</b>
<b>1 Introduction</b>	<b>1</b>
1.1 Research Question . . . . .	2
1.2 Thesis Outline . . . . .	3
<b>2 Constellation Design</b>	<b>5</b>
2.1 Coverage Overlap . . . . .	7
2.2 Revisit Time . . . . .	10
2.3 Further Remarks . . . . .	14
<b>3 Scheduling Approaches</b>	<b>16</b>
3.1 Constellation Scheduling . . . . .	16
3.2 Dynamic Scheduling . . . . .	17
3.3 Alternate Approaches . . . . .	18
<b>4 Model Architecture</b>	<b>21</b>
4.1 Use Case Analysis . . . . .	22
4.2 Model Description . . . . .	25
<b>5 OT-Scheduling-Service Implementation</b>	<b>29</b>
5.1 Order Types . . . . .	30
5.2 Scheduling Workflow . . . . .	31
5.2.1 Macro Scheduler . . . . .	33
5.2.2 Solver . . . . .	37
<b>6 Scheduling Results</b>	<b>38</b>
6.1 OroraTech Constellation . . . . .	38
6.2 One Orbital Plane . . . . .	40
6.3 Two Orbital Planes . . . . .	42
6.4 Four Orbital Planes . . . . .	44
6.5 Random Constellation Design . . . . .	47
6.6 Comparison . . . . .	49
<b>7 Conclusion</b>	<b>50</b>
<b>8 Outlook</b>	<b>52</b>

<b>A Appendix</b>	<b>53</b>
A.1 Full Use Case Analysis . . . . .	54
<b>Bibliography</b>	<b>55</b>

# List of Figures

1.1	Imaging data captured by FOREST-1 over the Sacramento Valley in California during the summer of 2022 split into the two imaging bands LWIR on the left and MWIR on the right, showing two hot spots in the MWIR band. . . . .	1
1.2	Infrared images captured by FOREST-1 of two active wildfires in California in the Sacramento Valley during the summer of 2022 demonstrating the characteristics of both infrared imaging bands layered on top of a regular RGB satellite image. . . . .	2
2.1	Visualizations of an exemplary Walker Delta constellation with a configuration of 9/3/2 next to a 5-2 <i>Flower Constellation</i> . . . . .	5
2.2	The FOREST-2 satellite carrying the next generation of the OroraTech thermal-infrared imager next to a render of the conception for the size and shape of the future OroraTech constellation. . . . .	7
2.3	Visualization of the accessible swath width by one satellite within the constellation right before an overpass over California with another satellite on a different orbital plane also visible in the background. . . . .	8
2.4	Graphs for the coverage overlap between the footprints of two adjacent satellites within the same orbital plane plotted against the number of satellites per plane for orbit heights of 300, 550, and 700km. . . . .	9
2.5	Exemplary ground tracks for a constellation featuring eight satellites in one orbital plane. . . . .	10
2.6	Visualization of the ground tracks of an exemplary satellite constellation with 16 satellites spread out over four orbital planes, plotted in STK. . . . .	11
2.7	Maximum Revisit Time in hours plotted against the number of satellites within a satellite constellation evaluated for the cases of one, two or four equally spaced orbital planes. . . . .	13
2.8	Graph with the number of planes with eight satellites each plotted against the maximum revisit time, including theoretical estimates. . . . .	13
4.1	Diagram depicting the most important use cases stated at the beginning of this work. . . . .	24
4.2	Illustration how the different commands, execution times and margins constitute an imaging window and book a certain period of available on-orbit time of the satellite. . . . .	27
5.1	Block definition diagram illustrating all implemented components of the OT-scheduling-service. . . . .	29
5.2	Use Case diagram to illustrate the potential application types of both order types. . . . .	30
5.3	Activity diagram illustrating the overall workflow of the OT-Scheduling Service for new incoming and pending orders and periodic automated schedule generation. . . . .	32
5.4	Comparison between the two stages of importing an AOI target into the set of permanent imaging targets of the <i>Macro Scheduler</i> . . . . .	33
5.5	Activity diagram illustrating the overall workflow of the OT-Scheduling Service for new incoming and pending orders and periodic automated schedule generation. . . . .	35
6.1	Results for on-orbit time allocation from the scheduling result for the current OT constellation. . . . .	39
6.2	Results for on-board storage allocation from the scheduling result for the current OT constellation. . . . .	39
6.3	Results for on-orbit time allocation from the scheduling result for the scheduling scenario of one orbital plane with eight satellites. . . . .	41



6.4	Results for on-board storage allocation from the scheduling result for the scheduling scenario of one orbital plane with eight satellites. . . . .	41
6.5	Results for on-orbit time allocation from the scheduling result for the scheduling scenario of two orbital planes with a difference in RAAN of $90^\circ$ with eight satellites each. . . . .	43
6.6	Results for on-board storage allocation from the scheduling result for the scheduling scenario of two orbital planes with a difference in RAAN of $90^\circ$ with eight satellites each. . . . .	43
6.7	Results for on-orbit time allocation from the scheduling result for the scheduling scenario of four orbital planes with a difference in RAAN of $45^\circ$ with eight satellites each. . . . .	45
6.8	Results for on-board storage allocation from the scheduling result for the scheduling scenario of four orbital planes with a difference in RAAN of $45^\circ$ with eight satellites each. . . . .	46
6.9	Results for on-orbit time allocation from the scheduling result for the scheduling scenario of eighteen satellites with each on its own orbital plane with the set of planes randomly spaced between them. . . . .	48
6.10	Results for on-board storage allocation from the scheduling result for the scheduling scenario of eighteen satellites with each on its own orbital plane with the set of planes randomly spaced between them. . . . .	48
A.1	WIP Update this with a diagram that shows only the discussed use cases which are actually related to the scheduler component/ Description of graphic. . . . .	54

# List of Tables

5.1	Imaging Opportunities Matrix Notation . . . . .	36
6.1	Comparison Scheduling Results . . . . .	49

# Acronyms

- ADCS** Attitude Determination and Control System. 27
- AEOs** Agile Earth Observation Satellites. 18
- AI** Artificial Intelligence. 52
- AOI** Area of Interest. viii, 30, 33, 38
- API** Application Programming Interface. 31, 33
- APIs** Application Programming Interfaces. 17, 31
- COIN-OR** Computational Infrastructure for Operations Research. 37
- ConOps** Concept of Operations. 16, 17, 51
- DRL** Deep Reinforcement Learning. 19
- ECEF** Earth-Centered, Earth-Fixed. 6
- EO** Earth Observation. 1, 3, 5, 6, 10, 14–19, 29, 47, 50, 52
- ESA** European Space Agency. 16
- FSS** Federated Satellite Systems. 14
- GPS** Global Positioning System. 14
- GSD** Ground Sampling Distance. 17
- LEO** Low Earth Orbit. 5, 6, 9, 11, 16, 18, 47, 50
- LEOP** Launch and Early Orbit Phase. 31
- LWIR** Long-Wave Infra-Red. viii, 1
- MC** Mission Control. 3, 19, 30, 33, 37
- MEO** Medium Earth Orbit. 14
- MILP** Mixed-Integer Linear Programming. 17, 37
- MWIR** Mid-Wave Infra-Red. viii, 1
- OT** OroraTech. viii, 1–3, 6, 9, 11, 21, 22, 25, 26, 28–33, 35, 37–39, 50–52
- PuLP** Python Linear Programming. 37
- RAAN** Right Ascension of the Ascending Node. ix, 8, 9, 11, 38, 42–46

**REST** Representational State Transfer. 31

**RGB** Red-Green-Blue. viii, 1, 2, 26, 33

**SSO** Sun-Synchronours Orbit. 6, 9, 17

**STK** Systems Tool Kit. viii, 6, 11, 18

**TLE** Two-Line Element. 11, 31

**WFS** Wildfire Solution. 1, 25

# 1 Introduction

Munich-based Earth observation company OroraTech (OT) has launched its second thermal-infrared imager into space on-board the FOREST-2 satellite. As a global leader in space-based thermal intelligence, OroraTech (OT) announced the beginning of their global thermal intelligence service in [1]. The thermal infrared imagers designed and built by OT feature recordings of the earth both in Long-Wave Infra-Red (LWIR) and Mid-Wave Infra-Red (MWIR) bands as well as Red-Green-Blue (RGB) imaging. The capabilities of the in-orbit demonstrator FOREST-1, predecessor of the FOREST-2 satellite, are illustrated in Figure 1.1a and Figure 1.1b. The illustration shows both bands next to each other with two visible bright spots in the MWIR image. Matching the detections with the available data in OT's Wildfire Solution (WFS), OroraTech (OT) identified both of these bright spots as active wildfires. Wildfire Solution (WFS) is the data product platform developed by the company for early wildfire detection. The platform is built on top of satellite data that is already available. The complete result can be seen in Figure 1.2, where the LWIR image is layered on top of a regular map of California with two cutouts for displaying the detected hot spots in the MWIR band.

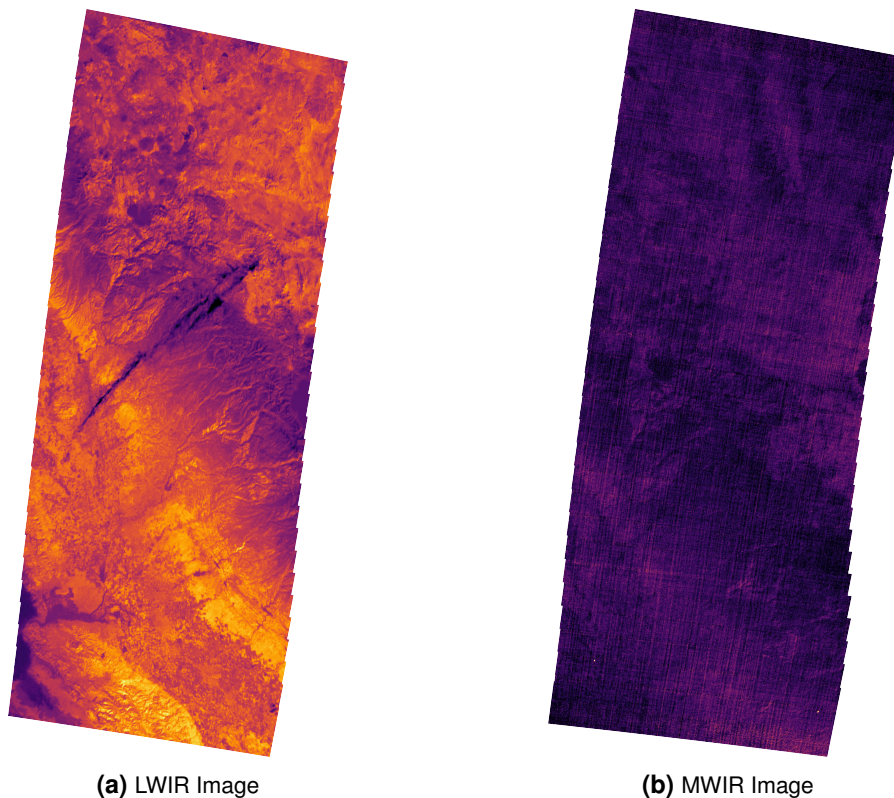


**Figure 1.1** Imaging data captured by FOREST-1 over the Sacramento Valley in California during the summer of 2022 split into the two imaging bands LWIR on the left and MWIR on the right, showing two hot spots in the MWIR band.

The objective of OT is to shift from utilizing available satellite data to utilizing thermal-infrared data obtained from its own constellation of satellites. Therefore, OT will need to design and implement an approach to their mission operations to efficiently command their fleet of Earth Observation (EO) satellites. In order to maximize the output and return on valuable data for exploring and servicing use cases ranging from wildfire early detection and monitoring, identifying urban heat islands, or observing sea surface temperature, there

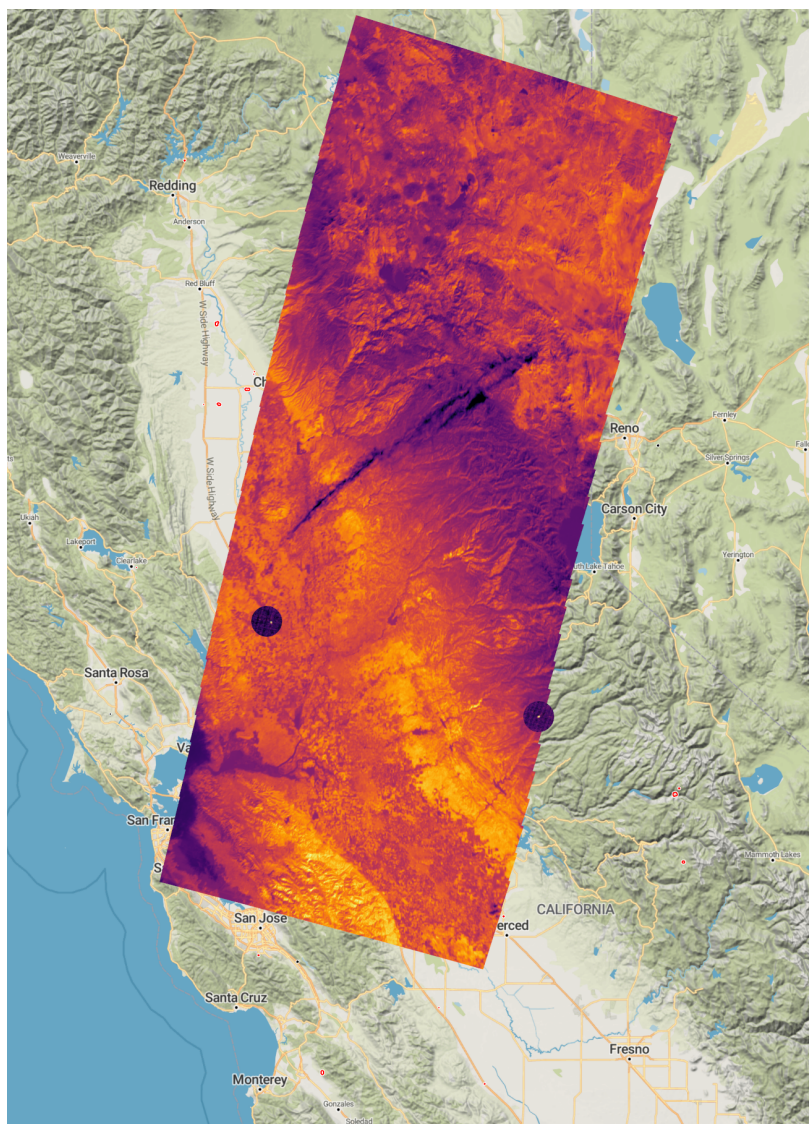


**Figure 1.2** Infrared images captured by FOREST-1 of two active wildfires in California in the Sacramento Valley during the summer of 2022 demonstrating the characteristics of both infrared imaging bands layered on top of a regular RGB satellite image.

is a compelling case to be made in favor of an optimized approach to the scheduling of its imaging activities and their satellite operations overall. Ideally, the approach will utilize the constellation design to achieve a revisit time of less than thirty minutes for all locations on Earth, as stated by the company in [2].

## 1.1 Research Question

This thesis shall describe and explain the steps that were taken over the course of developing the payload scheduling component of the OT-scheduling-service, an order-based automated solution for handling a vast selection of targets and requests that is designed to maximize the amount of high-quality data via optimizing the corresponding resource allocation. Coordinating imaging activity for incoming requests on top of permanent imaging targets is time-consuming for human operators, as demonstrated during operations of FOREST-1. This process generally follows the same steps each time. Therefore, it has been identified as a prime candidate for automation. Even more, due to the growth in complexity of the scheduling problem due to the recent launch of FOREST-2 and the launch of the first orbital plane carrying

eight more satellites scheduled before the end of 2024. At the same time, algorithm-based resource allocation solutions have shown to significantly outperform Mission Control (MC) personnel.

This thesis shall answer the following central research question: us,

- How do the size and shape of a heterogeneous Earth observation satellite constellation affect its performance with regard to an optimized scheduling approach?

In order to answer this question comprehensively, basic principles in satellite constellation design will be introduced and evaluated in particular with regard to:

- How can constellation performance parameters be selected and tailored towards a specific set of mission goals and requirements?
- How does the size, the total number of satellites, influence the coverage capabilities of an Earth Observation (EO) satellite constellation?
- How can the shape, the number of, and distribution among different orbital planes, assist in improving constellation performance?

Further, the presented architecture of the model and implementation of the scheduling approach will target answering:

- How is the scheduling of the constellation affected by these design parameters, especially with respect to the average resource allocation and the ability to fulfill a given set of imaging orders for different constellation design scenarios?

## 1.2 Thesis Outline

This thesis is structured as follows:

- Section 2 Constellation Design presents an introduction to the basics of satellite constellation design, in particular, two methodologies for the overall design and two candidates as possible constellation performance parameters are presented. The orbit design parameters discussed in this thesis include the inclination, orbit height, coverage overlap, and the revisit time.
- Section 3 Scheduling Approaches presents an overview of a selection of existing approaches to optimizing the scheduling of satellite constellations in the context of their respective use cases. In addition, dynamic scheduling approaches and some examples of solutions to a scheduling problem outside of the satellite context are also introduced.
- Section 4 Model Architecture introduces the model architecture that has been developed over the course of this thesis starting with a use case analysis to determine the environment and its interfaces, describing the mathematical model itself and the approach to solving the underlying problem.
- Section 5 OT-Scheduling-Service Implementation consequently provides an overview of the actual implementation of the work done within the scope of this thesis into the OT scheduling service, including the overall scheduling workflow on an architecture level.
- Section 6 Scheduling Results presents the results of the optimization efforts performed by the implemented scheduler for a selection of constellation configurations. This section shall demonstrate how changing the number of satellites per plane and orbital planes affects the frame in which the scheduler is able to operate.
- Section 7 Conclusion provides a concluding statement about how the optimization of schedules for a heterogeneous EO constellation is affected by its size and shape.

- Section 8 Outlook concludes this thesis with a prospect on how the presented work might be continued in the future.

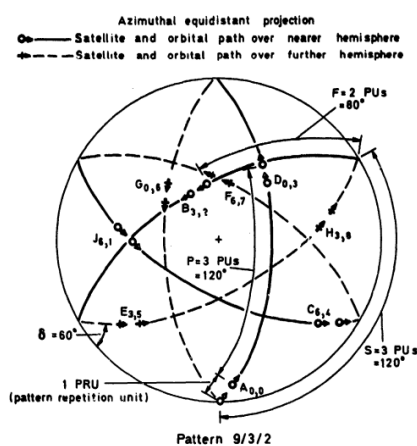


## 2 Constellation Design

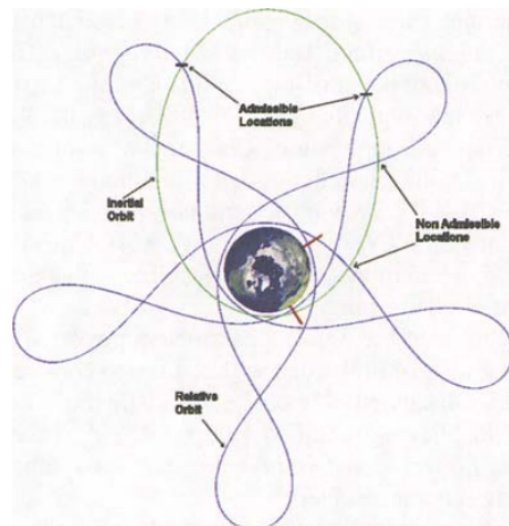
In the early stages of a mission, there are some key decisions to be made to set the general direction for the subsequent design work in order to achieve mission success in the most resource-effective manner. Within the field of Earth observation missions, the trade-off between deploying a single satellite and employing a dedicated constellation of satellites is of considerable importance. In general, choosing a constellation is rooted in the fact that they offer capabilities that are simply beyond the reach of single-satellite mission approaches, as put by Indrikis and Cleave in [3].

For the scope of this thesis, the assumption stands that a constellation of to-be-defined shape and size with respect to the total number of satellites and orbital planes in LEOs on which these are spread out is the favorable design option to fulfill the given mission goals. Nevertheless, there is a variety of constellation design patterns to choose from.

One design pattern that is frequently used as a reference for EO application is the Walker delta pattern. As presented by Walker in [4], each configuration is represented by three parameters under the assumptions of an identical inclination  $i$  for every orbital plane. According to Walker's notation presented in [5], an exemplary constellation configuration  $T/P/F$  shall be read as a constellation which in total consists of  $T$  satellites uniformly spread out across a number of  $P$  orbital planes with their ascending nodes with a phasing parameter  $F$ . This phasing parameter specifies the shift between satellites in their ascending node in adjacent orbital planes. Figure 2.1a illustrates how a  $9/3/2$  Walker delta pattern with an inclination  $i = 60^\circ$  for all three of its orbital planes would look like. The key design paradigm behind Walker constellations is seen as the uniform distribution of the total number of satellites within the constellation across the desired number of orbital planes. The objective is to establish uniform coverage.



(a) Illustration of a Walker constellation with a delta pattern of  $9/3/2$  showing nine satellites spread out across three orbits, with the reference plane viewed from above.[5]



(b) Visualization of a 5-2 *Flower Constellation* showing two satellites with five petals with the characteristic phasing.[6]

**Figure 2.1** Visualizations of an exemplary Walker Delta constellation with a configuration of  $9/3/2$  next to a 5-2 *Flower Constellation*.

Another methodology for the design of a satellite constellation, the *Flower Constellations*, has been presented by Mortari, Wilkins, and Bruccoleri in [6]. These constellations are composed of a series of repeating ground tracks that are combined with a suitable phasing mechanism. Similar to a Walker delta pattern, there are also three design parameters to specify a *Flower Constellation*: the number of petals  $N_p$ , the number of sidereal days it takes for the ground track to repeat  $N_d$  and the total number of satellites  $N_s$ . Besides these, the argument of perigee  $w$ , inclination  $i$ , and the altitude of the perigee  $h_p$  are the same for every satellite within the constellation. Contrary to other constellation designs, in *Flower Constellations*, all assets follow one trajectory with respect to a rotating reference frame. Hence, the flower-like patterns develop for projections of these intricate trajectories. Since most orbit visualization tools rely on an Earth-Centered, Earth-Fixed (ECEF) coordinate system, e.g. STK offered by AGI at [7], and therefore lack the capabilities to illustrate these characteristic orbit shapes, further research presented by Bruccoleri and Mortari in [8] filled the need of dedicated visualization tools for *Flower Constellations*. The result of this becomes visible in Figure 2.1b, where the visualization of a 5 – 2 *Flower Constellation* illustrates the trajectory for two satellites passing through the five petal-shaped formations.

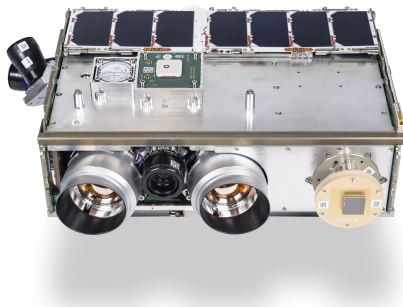
Therefore, these forms of constellations are applicable to a variety of mission objectives, including EO, global navigation or in general objectives that profit from the achieved symmetry, as declared by Avendaño, Davis, and Mortari in [9]. Moreover, it is in principle also possible to re-orientate such a constellation. However, that maneuver would require continuous active control to maintain its constellation performance.

Further research conducted by Arnas et al. in [10] proposes a *slotting system* for collision avoidance in LEO. Due to the symmetric properties of flower constellations and therefore favorable behavior in this regard, the authors were able to investigate the limit of how many satellites could theoretically co-exist in LEO in the context of multiple emerging mega-constellations.

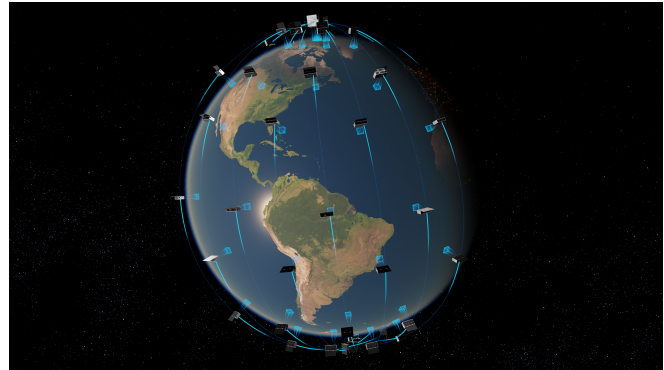
unlike satellites in geostationary orbits, which are fixed in their position relative to Earth, as described by Walter in [11], satellites in a LEO generally offer coverage of more than a fixed region on ground due to characteristically short orbital periods. The visible area of a non-geostationary satellite is determined by its inclination angle ( $i$ ), which indicates the highest theoretically visible latitude. Orbits with an inclination  $i$  of exactly ninety degrees are referred to as *polar* orbits and ones with inclinations around  $i = 98^\circ$  are known as Sun-Synchronous Orbit (SSO). Thus, for EO missions, the choice of orbit inclination is directly related to the type of targets that are specified in the mission requirements.

At the same time, they present a comparatively cheap and accessible option due to the constantly growing availability of rideshare launches, as for example advertised by SpaceX in [12]. Combined with the advancements made in scaling down earth observation instruments to fit in with the class of micro- and nanosatellites, as it has been demonstrated and published e.g. by companies such as ICEYE in [13] or OroraTech in [14], EO constellations in LEO provide a cost-effective option for a wide range of missions. Below, Figure 2.2 showcases the most recent CubeSat development of OroraTech's thermal-infrared imager integrated into the FOREST-2 satellite, a 6U CubeSat, next to an illustration of the scale and shape of the projected future constellation, whose first plane is scheduled to launch in 2024, where each satellite will carry the same version of the instrument. The constellation design of OT targets operating and maintaining a constellation of around ninety-six satellites spread out across multiple orbital planes with eight satellites each. As reported by Spacenews in [15], the Falcon 9 rocket by SpaceX carried over seventy satellites, including FOREST-2, as a dedicated rideshare mission for small satellites into LEO. This news, along with the observable trend of scaling down spacecraft sizes while simultaneously offering launches without primary large spacecraft, clearly emphasizes the increasing availability and accessibility of space technology.

There are various methods to evaluate the performance of a satellite constellation. The most common one is coverage, which refers to different interpretations, as described by Larson and Wertz in [16]. Nevertheless, the unique needs of different EO missions, such as the time gap between data acquisition and delivery to the end-user, or the period between two acquisitions of the same area, known as latency and revisit period, vary significantly. Due to these variations, there cannot be a single metric to determine



(a) The FOREST-2 satellite.



(b) The Future OroraTech Constellation.

**Figure 2.2** The FOREST-2 satellite carrying the next generation of the OroraTech thermal-infrared imager next to a render of the conception for the size and shape of the future OroraTech constellation.

the performance of a constellation accurately in any situation. Consequently, such aspects necessitate a detailed study of the primary factors that determine the success of each mission individually.

For this thesis, two parameters have been identified to assess the performance of a heterogeneous Earth observation satellite constellation: coverage overlap and revisit time. These parameters will be used to determine the ideal size and shape of the satellite constellation. These include and will be referred to in the following subsections as coverage overlap and revisit time and will be concluded by remark on further considerations.

This section introduces and evaluates these two different measures for assessing the performance of a heterogeneous Earth observation satellite constellation with respect to their suitability and their sensitivity to the size and shape of exemplary constellation designs. Whenever a tangible exemplary mission is required to demonstrate the dependencies among different parameters, the previously introduced existing constellation of thermal-infrared imaging constellation developed and hosted by OroraTech shall be used as the starting point.

## 2.1 Coverage Overlap

The overall process of setting up an Earth observation constellation comes down to incrementally increasing its capabilities over multiple launches. Deploying the full constellation simultaneously is not practical or commercially viable in most cases, particularly when it requires satellites on multiple orbital planes. Multiple launches enable more development iterations of the satellite platform and its instruments are possible and the overall risks can be reduced significantly. This equally accelerates the process of having and operating satellites in orbit earlier by a significant margin.

Therefore, a first step might be to close the gap between two adjacent ground tracks, including the swath of the respective imaging instruments, within the same orbital plane. As illustrated in Figure 2.3, this gap is closed once the cones demonstrating the instrument's swath width touch and overlap with each other for two adjacent satellites. By closing these gaps, the theoretically achievable coverage becomes continuous and thereby the constellation becomes capable of observing any location on Earth within one orbital period. This assumption, however, is limited by the actual concept of operations, which also takes into account reserving operations time for sun-pointing, in order to maintain a positive power budget, ground station contacts, or any other maneuvers that diverge from nominal procedures.

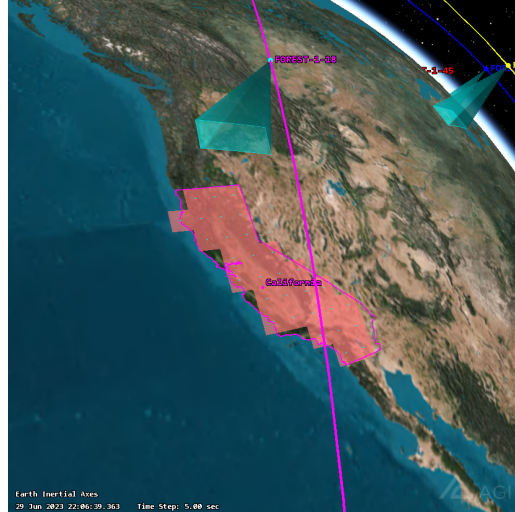


**Figure 2.3** Visualization of the accessible swath width by one satellite within the constellation right before an overpass over California with another satellite on a different orbital plane also visible in the background.

This design parameter is dictated by the specifications of the instrument itself and the characteristics of the chosen orbit, namely the inclination  $i$  and the orbital period  $T_{orb}$ . The goal of this approach is to balance out the displacements of the ground tracks caused by the Earth's rotation itself and the shift of the Right Ascension of the Ascending Node (RAAN)  $\dot{\Omega}$ , both dependent on the time that passes between two adjacent satellites in the same orbital plane, referred to as  $t_{revisit}$  in Equation 2.2, and an overlap between the distances covered by the swath width  $w_{swath}$  of each instrument at the equator. Taking both of the mentioned influences into account, the total displacement  $d_{total}$  at the equator is defined as:

$$d_{total} = 2\pi R_{\oplus} \cdot t_{revisit} \cdot \left( \frac{1}{T_{sid}} - \frac{\dot{\Omega}}{2\pi} \right) \quad (2.1)$$

$$t_{revisit} = \frac{T_{orb}}{n_{sats}} \quad (2.2)$$

The width of the footprint of the instrument at the equator  $d_{swath}$  varies with the inclination  $i$  of the chosen orbit and is calculated as shown in Equation 2.3. However, the difference in  $d_{swath}$  for different inclinations for the same orbit heights has turned out to be negligibly small and was therefore not further investigated. Here, the equator is chosen as the point of reference as the distance between two ground tracks reaches its maximum there and only gets smaller the more the latitude diverges from zero.

$$d_{swath} = \frac{w_{swath}}{\sin(i)} \quad (2.3)$$

Following the derivation presented by Assmann in [17], the minimum number of satellites required per plane  $n_{sats,min}$  to create an overlap between the distances which the instruments of two adjacent satellites cover on ground, is calculated as follows:

$$n_{sats,min} = 2\pi R_{\oplus} \cdot \frac{T_{orb} \cdot \sin(i)}{w_{swath}} \cdot \left( \frac{1}{T_{sid}} - \frac{\dot{\Omega}}{2\pi} \right) \quad (2.4)$$

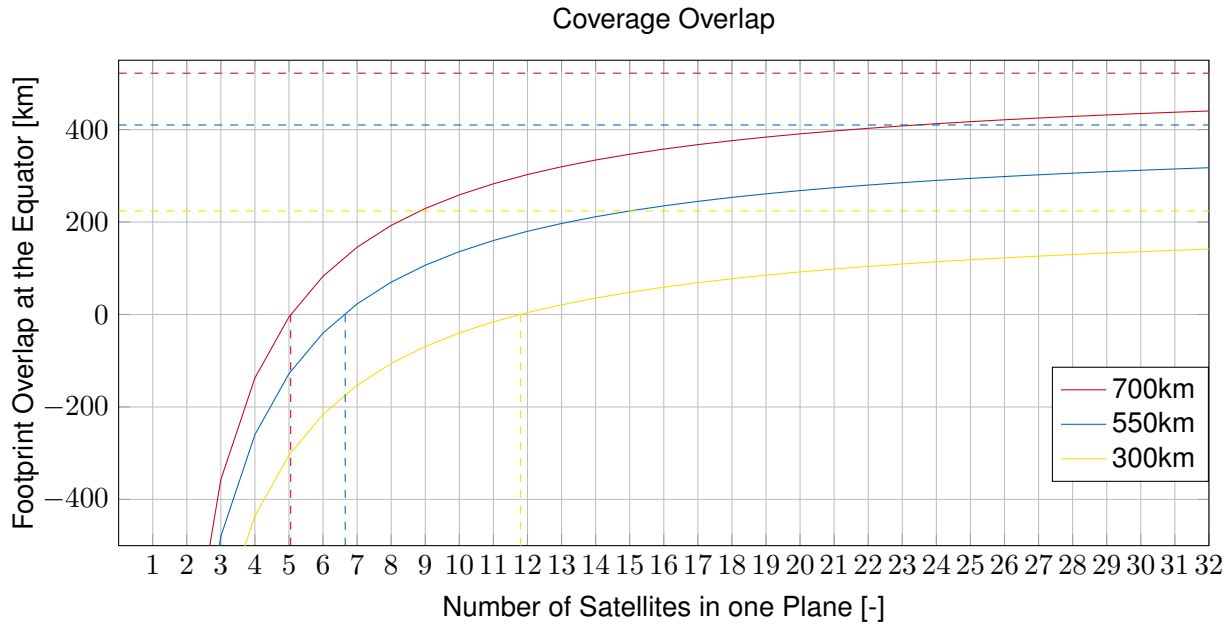


**Figure 2.4** Graphs for the coverage overlap between the footprints of two adjacent satellites within the same orbital plane plotted against the number of satellites per plane for orbit heights of 300, 550, and 700km.

with the shift of the RAAN  $\dot{\Omega}$  defined as:

$$\dot{\Omega} = -\sqrt{\frac{\mu}{a^3}} \cdot \frac{3}{2} \cdot J_2 \cdot \left[ \frac{R_{\oplus}}{a \cdot (1-e)^2} \right] \cdot \cos(i) \quad (2.5)$$

Evaluating the achievable ground track overlap for an exemplary constellation in LEO at an orbit height of 550km, carrying the FOREST-2 imaging instrument, yields the graph depicted in Figure 2.4. Additional plots have been added for different orbit heights to illustrate the coverage overlap's sensitivity for other LEOs. With different orbit heights, most importantly the width of the footprint on ground  $w_{swath}$  will change. The assumptions here include an ideal circular orbit, so an eccentricity  $e$  equal to zero. Thus, the semi-major axis  $a$  results directly from adding the orbit height to the Earth's radius  $R_{\oplus}$  of 6371km. In order to reach the intended Sun-Synchronous Orbit (SSO) for the future OT constellation, the inclination  $i$  is set at 98°. Earth's gravity parameter  $\mu_{\oplus}$  is set to  $3.986 \cdot 10^{14} \frac{m^3}{s^2}$  and the second harmonic coefficient  $J_2$  to 0.0010826267, both constants. Furthermore,  $T_{orb}$  and  $T_{sid}$  reflect the orbital period of each satellite and the duration of one sidereal day, respectively.

There are multiple aspects worth mentioning about the depicted graphs. Firstly, for the targeted configuration, there is overlap for any constellation design with orbit heights of 300km, 550km, and 700km that features more than eleven, six, or five satellites per plane, respectively, as indicated by the vertical dashed lines. Secondly, the improvement in terms of how far the overlap reaches shows the clearly visible tendency to flatten out for large numbers of satellites, in each asymptotically converging towards the respective swath width  $w_{swath}$ . The swath width  $w_{swath}$  is indicated by the horizontal dashed lines in the corresponding color. This effect is visible throughout all orbit heights, even though an overlap is visible earlier or later for higher or lower LEOs.

Therefore, at some point, this measure for constellation performance loses its significance. Adding more satellites to the same orbital plane beyond the respective threshold for creating an overlap in coverage does not offer a significant gain in performance for the chosen metric. The resulting design shall still account for satellites dropping out of the constellation for certain periods of time or permanently with accordingly defined margins for the number of satellites per plane. Once this point has been reached, considering ground track overlap alone does not provide a comprehensive overview. Most significantly, this measure

is limited to evaluating one orbital plane at a time. Hence, any effects a constellation configuration with more than one plane might or might not benefit from employing multiple planes cannot be captured. In conclusion, this measure is a viable metric for the minimum number of satellites per plane, especially during the incremental process of building up a EO constellation, but lacks the capabilities to further evaluate constellation performance beyond a single orbital plane.

## 2.2 Revisit Time

Another measure to assess the performance of an EO constellation widely employed is its revisit time, which in principle refers to the period of time that passes between two subsequent overpasses of at least one satellite over the same location. Due to the orbital mechanics of satellite constellations, this period is not strictly the same for each pair of overpasses and therefore multiple interpretations of the term revisit time are in use. Among other candidates for a *coverage figures of merit*, Larson and Wiley introduce the *Maximum Coverage Gap* in [16] as one interpretation of revisit time. This term plainly relates to the maximum period of time between two overpasses over a specific location on ground.

In some cases, using an average of these periods to assess overall constellation performance might provide a broader overview. However, since revisit times are invariably related to individual targets, the average shows a tendency to blur the shortcomings of the overall constellation design.

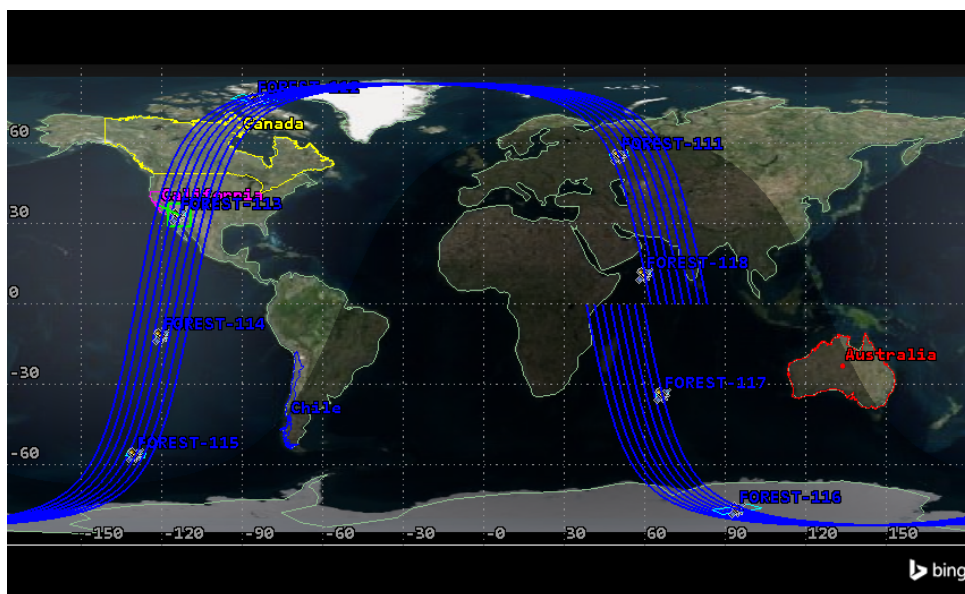


**Figure 2.5** Exemplary ground tracks for a constellation featuring eight satellites in one orbital plane.

The reason for this can be deduced from the illustration above. Figure 2.5 shows a visualization of the groundtracks of an exemplary constellation of eight satellites, all within the same orbital plane. This demonstrates how the revisit time between overpasses of adjacent satellites can be adjusted by the number of satellites within the same plane, as introduced in section 2.1. However, the number of satellites is not capable of closing the clearly visible large gap between the two bundles of satellite ground tracks as these are bound to the orbit itself. Thus, reducing the maximum revisit time of a satellite constellation has to be realized via employing multiple orbital planes.

Achieving maximum revisit times below a certain threshold might prove to be crucial in certain satellite constellation mission goals. Especially for disaster management applications, such as designing a satellite constellation for the purpose of early wildfire detection, this measure takes on a central role. The longer such events go undocumented due to large coverage gaps, the longer the corresponding response will be delayed. In this regard, Buzzi et al. in [18] performed an exhaustive investigation for a range of eligible

figures of merit to determine the performance of the constellation that was designed for the Time-Resolved Observations of Precipitation structure and storm Intensity with a Constellation of SmallSats (TROPICS) mission. In their work, the authors equally identified the weakness in using averages for coverage gaps, which are commonly referred to as revisit times within the scope of this work, due to their resulting oversight of long periods without any coverage.

Given that computing the revisit time of a satellite constellation in LEO for a specific target does not have a straightforward analytical solution, AGI's Systems Tool Kit (STK) from [7] was chosen as the simulation tool to assess the effects of changing the shape and size of the constellation for an exemplary target. In this case, the simulation was set up to compute the *Maximum Revisit Time*, which was evaluated via the *Coverage Definition* feature in STK. The seed satellite for this case was defined according to the design of OT's FOREST-2 imager on an ideal circular orbit with a swath width  $d_{swath} = 400km$ , an orbit height  $h = 550km$ , and an inclination  $i = 98^\circ$ . Exemplary values for the RAAN, true anomaly and the argument of perigee were pulled from the corresponding Two-Line Element (TLE) but do not present a significant contribution to the revisit time. The simulation was carried out for the seed satellite alone, and afterwards constellation configurations featuring four, eight, sixteen and thirty-two satellites spread out over one, two or four orbital planes respectively. The spacing between and on each of these orbital planes was assumed to be uniform.

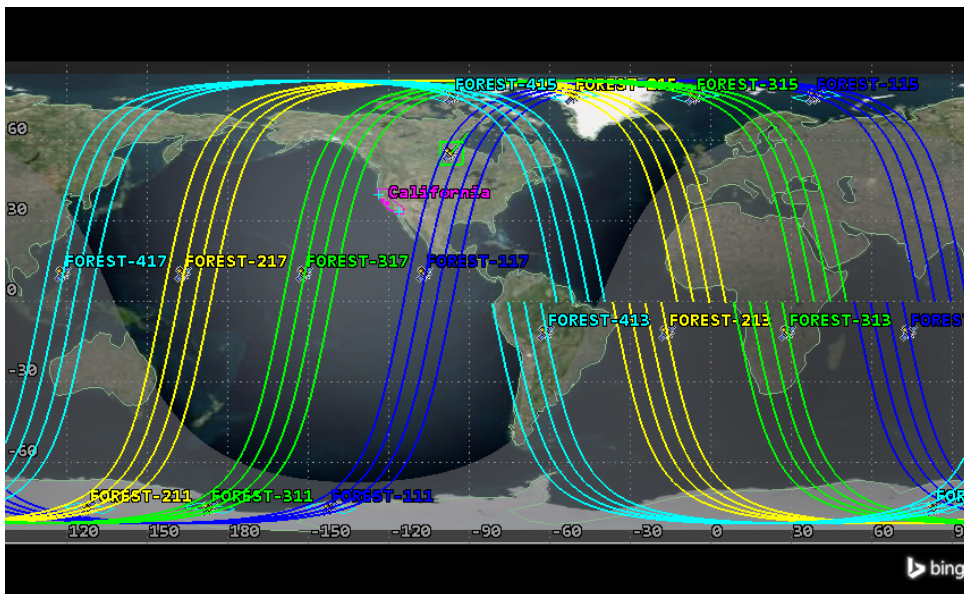


**Figure 2.6** Visualization of the ground tracks of an exemplary satellite constellation with 16 satellites spread out over four orbital planes, plotted in STK.

The results of these simulation runs are presented below in Figure 2.7. Further, the ground tracks of the configuration featuring sixteen satellites in four equally spaced orbital planes is also illustrated in Figure 2.6. The ground track visualization demonstrates the effect of adding orbital planes to a constellation design, namely closing the gaps in coverage between the groups of ground tracks. The results for one single orbital plane show how increasing the number of satellites in one plane alone does not show any noteworthy improvement. Moreover, the trend follows the same behaviour which has been presented earlier in section 2.1 regarding the flattening out of increasing an overlap in the footprint between two adjacent satellites within the same orbital plane.

However, as can be seen in Figure 2.7, distributing the same number of satellites among more orbital planes does not necessarily improve the maximum revisit time. Especially the evaluation case for eight total satellites demonstrates the decline in performance if only one design directive is considered. Revisiting the argument for more than seven satellites per plane introduced in section 2.1, lowering the number of satellites per plane and arranging them in multiple planes re-opens the gap in adjacent footprints within

the same orbital plane. Therefore, targets on ground might not be covered with every overpass of the bundle of ground tracks of a single orbital plane. Consequently, this influences the maximum revisit time in a negative manner. The same argument can be made for comparing e.g. only the scenarios with the same number of planes with each other. The clear improvements from adding more satellites to the same number of planes can be observed for the steps that close the gap in coverage and tends to subside afterwards.

The graphs for a total number of thirty-two satellites however showcase that constellation configurations in which each orbital plane fulfills the requirement of continuous coverage exhibit the intended performance improvements. Adding additional equally spaced planes to the constellation helps to close the gaps which could be easily identified in Figure 2.5. Hence, another evaluation was performed to investigate how exclusively adding orbital planes with eight satellites each improves the maximum revisit time. The results are plotted in Figure 2.8. There, the simulation results for a number of one up to sixteen orbital planes are plotted together with the theoretical estimates, following the following equation for the maximum revisit time presented by Liu in [19]:

$$t_{revisit,max} = \frac{24h}{2 \cdot n_{planes}} \quad (2.6)$$

Both types of results follow the identical trend of achieving continuously better performance for an increasing number of orbital planes. The effect is most striking at the beginning, while it flattens out towards larger numbers of planes. Hence, once continuous coverage within each orbital plane could be established, adding more planes to the constellation is the preferred technique to improve this aspect of overall constellation performance. Moreover, Equation 2.6 proved to reliably produce a viable general estimate of the to-be-expected values. The consequently better results for the theoretical estimates can be deduced from the specific simulation setup, e.g. using regions at medium latitudes which are known to usually show slightly worse results for revisit time.



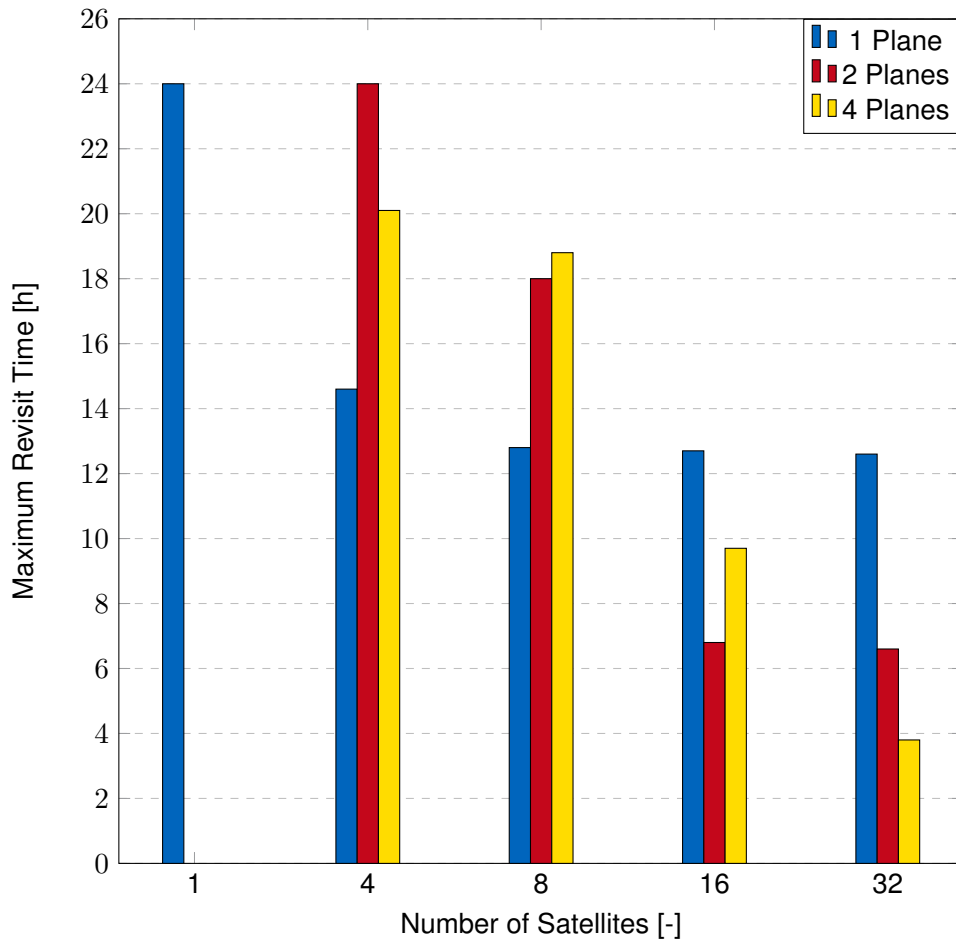


**Figure 2.7** Maximum Revisit Time in hours plotted against the number of satellites within a satellite constellation evaluated for the cases of one, two or four equally spaced orbital planes.

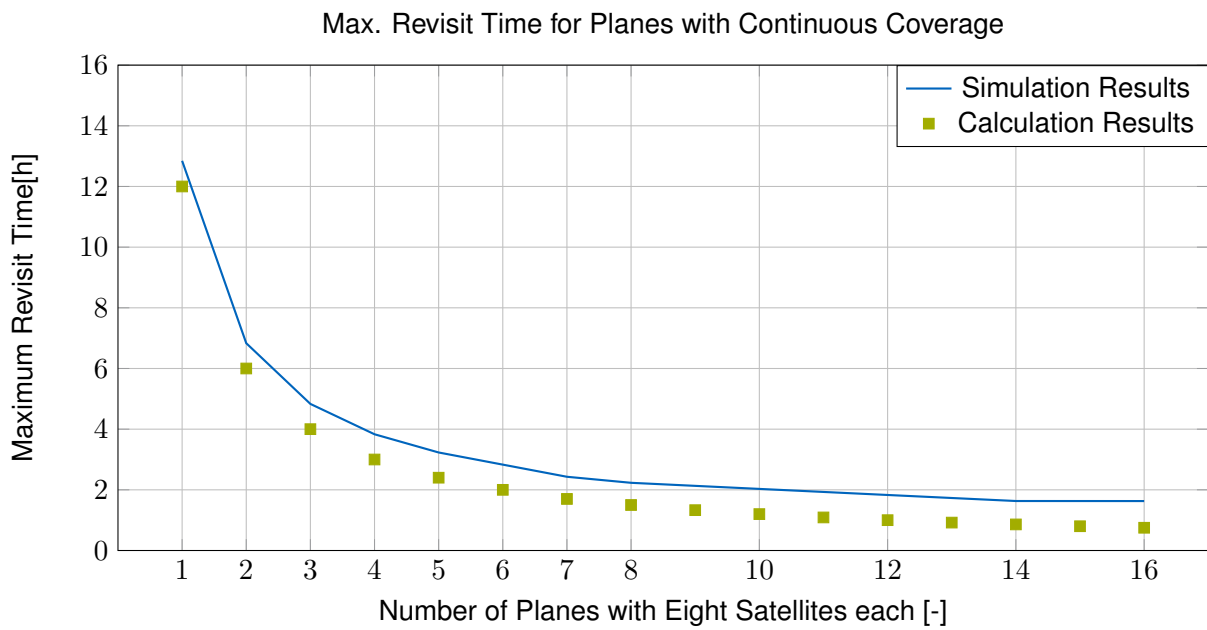


**Figure 2.8** Graph with the number of planes with eight satellites each plotted against the maximum revisit time, including theoretical estimates.

## 2.3 Further Remarks

In general, and as already stated in the introduction to this section, satellite constellation design is inevitably bound to a specific set of mission requirements and does not follow a clear guideline. However, the effects of adjusting size and shape of a constellation on its constellation performance, measured by a suitable figure of merit, are predictable. The two candidates to assess constellation performance discussed within this section shall provide an initial estimate for the number of satellites within one plane and the number of total orbital planes necessary to achieve a certain interpretation of coverage in an EO context. The presented results demonstrate the leverage available during design studies or early development phases.

Nevertheless, these considerations were taken under the assumption that one single observation by one asset at a time would be sufficient to establish coverage. This is not necessarily the case for all missions. As Zheng et al. illustrate in [20], once *multi-fold coverage*, coverage by more than one satellite at a time, becomes a requirement, the decisive parameters tend to shift to additionally include the orbit height as a decisive variable.

Furthermore, to reiterate on the exemplary scenario of disaster management applications of satellite constellations, design of the space segment of the constellation alone might not be sufficient in order to fulfil requirements which are formulated around latency. In this context, latency is commonly referred to as the time gap between the acquisition of a certain form of information, e.g. the detection of a rapidly spreading newly erupted wildfire, and the point at which this piece of information is available to its users on ground. Hence, the quality of the reaction on ground to time-sensitive information gathered by the satellite constellation in space is dictated by this aspect.

In theory, the gaps in between ground station contacts follow the same mechanics as relying on continuous coverage and aiming at lowering maximum revisit times, as introduced in section 2.1 and section 2.2 respectively. The only difference is that the target, in this case, would be an available ground station, potentially part of a larger ground station network, such as for example the global groundstation network offered and operated by Kongsberg Satellite Services (KSAT) in [21]. However, since at first any observation is limited to one specific satellite and not automatically to every asset within the constellation, latency does not coincide with the coverage gaps investigated earlier. Therefore, additional measures need to be taken to instrumentalize satellite constellation design not only for acquisition but also for the provision of data.

Extended research, such as the stakeholder analysis model presented by Golkar in [22], calls for the development of so-called *Federated Satellite Systems (FSS)* in order to have homogeneous satellite constellations evolve into distributed systems which would then be able to share in-orbit resources, especially capacities regarding their respective data and link budgets. This would in turn require the installment of dedicated *FSS-tailored ad-hoc networks* in order to facilitate this sort of resource exchange. Investigations conducted and presented by Sanad and Michelson in [23] on the other hand call for adding another layer to the constellation in the form of a communication relay constellation in Medium Earth Orbit (MEO) in order to cut down system response time, which corresponds to the latency term introduced earlier. This additional layer would benefit from the characteristic suitability of MEO for this sort of application, similar to how the constellation arrangement of the Global Positioning System (GPS) constellation described in [24] is able to offer almost complete coverage at all times while only using twenty-four satellites. Adding such a communication relay to an EO constellation equally creates a heterogeneous constellation design, which in turn constitute the theoretical boundaries within which subsequent mission operating and scheduling optimization can take place.

In conclusion, the findings with respect to constellation design of this thesis can be summarized as follows: In the beginning, there is an argument to be made to increase the number of satellites per plane until, including appropriate margins, an overlap in coverage is created. Afterwards, the design paradigm to follow in order to reduce revisit times for observation targets on ground has been identified as adding more orbital planes to the constellation. Both effects show a gradual decline after a certain point has been reached.

Breaking through these patterns requires further investigation of the mission goals and requirements for each instance separately. Preliminary design decisions with respect to the overall constellation design are generally made during the early design phases of a mission. Following this general mission progression, the next section will introduce an overview over a selection of scheduling approaches which in turn build on the underlying constellation design with the goal of extracting the optimal performance from a given constellation of EO satellites.

## 3 Scheduling Approaches

Once a project progresses beyond the early mission phases of identifying and developing a preliminary draft for the mission, following the well-established mission lifetime cycle as promoted by the European Space Agency (ESA) in [25], the basic constellation design is not expected to undergo major changes. Hence, in order to materialize the targeted constellation of an EO satellite constellation, the Concept of Operations (ConOps) has to be defined. With that, the approach to the scheduling itself becomes the interface where mission operations personnel decides on how the ground segment is supposed to interact with the space segment in order to capitalize on the available assets and their respective resources. On one hand, this includes allocating resources towards collecting the desired data from a set of targets via the satellite's payloads. On the other hand, it extends to delivering this data to ground in order for it to be distributed to its users. For the most part, these tasks tend to be repetitive but at also significantly time-consuming. This allows and calls for the highest possible degree of automation, in order to minimize cost and effort spent during nominal operations of a satellite constellation. Moreover, since the lifetime of satellite missions is limited, the time each asset spends operational in orbit shall be utilized as best as possible. Therefore, evaluating the scheduling of satellite constellations inevitably becomes an optimization problem, as well.

Considering the solution approaches for any sort of constrained optimization problem, the available body of literature is immense. Therefore, this section intends to present commonly used approaches and solving techniques for devising the scheduling of an EO satellite constellation. This thesis builds upon earlier work published in [26] which was performed on automating nominal payload operations for a single satellite, equally within a set of constraints on available resources. This section includes considerations regarding constellation scheduling in general and which approaches currently find application, dynamic scheduling and will additionally touch on successfully implemented methods outside the context of satellites in LEO or satellites altogether.

### 3.1 Constellation Scheduling

The scheduling of a constellation goes beyond applying the same approach that originally had been developed for a single satellite to each satellite within the constellation individually. Although most resources on-board the satellite cannot be shared between multiple spacecrafts, the scheduling has to take place in the context of the whole constellation in order to genuinely exhaust its capabilities of enhancing performance with respect to the mission success criteria.

In principle, each approach consists of a mathematical formulation of the scheduling optimization problem and some form of technique to solve the problem. Each model is structured in such a way that all criteria which are relevant for achieving greater contributions towards mission success are rewarded accordingly. Looking at prominent examples for scheduling large fleets of satellites, Cappaert et al. published an extensive overview of the optimizing efforts currently in use for the Spire constellation in [27]. Their model includes weights based on *latency*, *revisit*, *probability of detection*, *refresh* and *timeliness* which can be summarized via stating the goal as aiming at delivering quality imaging products of targets which are most likely to offer good conditions within the shortest time frame feasible. Scheduling solutions that are designed to encompass both payload activity and housekeeping tasks regularly face the issue of how to compare tasking of e.g. imaging against scheduling of ground station contacts. In the work of Cappaert and his co-authors, this problem is solved by multiple calls to the scheduling tool, which was purposely

designed for the Spire satellite constellation. This ensures that only tasks that are reasonably comparable are considered at the same time. The authors have achieved a solution that provides optimised scheduling results for a heterogeneous satellite constellation that is capable of handling any type of tasking that is expected to occur during nominal operations. In addition, the solution is complemented by a suite of Application Programming Interfaces (APIs) available to its customers, allowing them to access the centralized constellation scheduling product for tasking-based inputs.

Other efforts in automating mission operations for a constellation of satellites have been published by Mallik et al. in [28]. Their work dwells on the development of a system capable of automatically planning and executing any kind of maneuvers necessary to operate the SkySat constellation, hosted by Planet Labs. The SkySat constellation is composed of about twenty satellites capable of high-resolution imaging with a Ground Sampling Distance (GSD) of  $50\text{cm}$ , according to their description available at [29]. The SkySat constellation design includes both satellites in SSO as well as some in lower inclination orbits. The main focus of the presented initiatives is to reduce manual mission control workload and thus to make the management of the SkySat constellation more efficient in general. Due to the constellation design, nominal operations additionally include station keeping and occasional reconfiguration tasks. Thus, the proposed solution focuses on automatically determining when maneuvers are possible when certain maneuvers become mandatory, and during which times parts of the constellation are not operational, e.g. undergoing maintenance or other adjustments. Each maneuver planning is accompanied by an additional collision avoidance evaluation to mitigate risk and ensure smooth operations.

The formulation of the optimization problem is most commonly based on a Mixed-Integer Linear Programming (MILP) approach. Work published by Augenstein et al. in [30] presents the considerations made during the initial development of optimized schedules for the SkySat constellation. Most tasks for EO satellites can be assumed to be mutually exclusive. Therefore, preprocessing steps such as propagating the satellites' orbits to find upcoming imaging opportunities amount to a set of discrete entities. This allows to assign weights and resource requirements to each of these entities and formulate the optimization problem as maximizing the accumulated sum based on the attached figure of merit while staying within the pre-defined sets of constraints regarding available resources and technical hardware limitations. This technique of discretizing the scheduling of EO imaging satellites in this manner have also been demonstrated by Napallu et al. in [31], Bianchesi and Righini in [32] and Cho et al. in [33]. The strategies regarding the choice of algorithm to ultimately solve the optimization problem differ among this selection of literature but the discretization approach is noticeable in each.

Eddy and Kochenderfer argue in [34] that the choice of the algorithm offers an additional opportunity to optimize constellation performance. Besides a purely simulated example, the authors use the SkySat constellation as a test case in order to demonstrate how applying a graph-based solution approach can achieve higher performance within a quarter of the time. The objective function in this case equally relies on discretizing candidates for imaging activity. The authors furthermore state that the complexity scales exponentially with respect to the number of tasks and linearly with the number of available satellites within the constellation. Based on that, they argue that this creates an unmanageable workload for human operators which consequently calls for automation efforts for nominal spacecraft operations. Consequently, there were further research efforts devoted to the development of a whole suite of tools to automate mission operations for the SkySat constellation with regards to how they can help to reduce operator workload and at the same time enhance the overall level of constellation management, as also presented by Mallik et al. in [28].

## 3.2 Dynamic Scheduling

Satellite operations usually revolve around a baseline of nominal operations based on the respective ConOps. For EO missions, this consists of some form of an acquisition plan with a defined scheduling horizon for a set of imaging targets. The time frame of these acquisition plans can range from multiple

months, as shown by Arvidson in [35] for Landsat-7, to scheduling horizons of twenty-four hours, as practiced and demonstrated by Cappaert et al. in [27]. However, in the course of routine operations, these standing set of targets might prove to be insufficient. As a result, authors such as Pemberton and Greenwald in [36] expressed the *need for dynamic scheduling of imaging satellites*. This need is argued for with reference to the traditionally static nature of satellite scheduling as a process that purely revolves around the distribution of resources among a range of to-be-scheduled tasks. EO satellites in LEO offer a level of flexibility that exceeds the capabilities of being limited to a single or multiple areas of interest. Moreover, this allows for short-term adjustments as a direct response to unfavorable imaging conditions over certain targets, as described by Liao and Yang in [37]. Their work describes how to deal with customer requests for the single satellite FORMOSAT-2 with regard to optimizing imaging results based on predicted weather conditions. The scheduling problem was formulated in the context of orders issued by customers which would then in turn be processed by the scheduler, again in a discretized manner. There are plans for future constellation designs for scientific satellites to encompass a task request-based workflow into the continuous nominal imaging operations, as presented by Medina, Redfern and Talpas for the Polarimeter to UNify the Corona and Heliosphere (PUNCH) mission planning system in [38]. The produced approach combines a mission planning tool in order to determine suitable time slots for the requested tasks with the commercially available STK Scheduler to ensure conflict-free schedules. A more in-depth evaluation of the methodology behind the STK Scheduler is provided by Fisher and Herz in [39].

Dynamic scheduling is an integral part of any scheduling application to be used in emergency monitoring EO applications. Due to the time-constrained nature of the to-be-observed targets, it is imperative to account for these cases in the scheduling approach. In most cases, acquisitions of these events lose any significance once they are captured outside of this scope. Therefore, especially for disaster management use cases, there are noteworthy advances in the field of agile or dynamic scheduling models and algorithms. Sun et al. address the issue of merging an incoming imaging request for an active emergency situation into an existing optimized schedule in [40]. This approach builds on advances in the attitude control capabilities of new generations of satellites, referred to as Agile Earth Observation Satellites (AEOs) due to their capabilities of orienting the imaging instrument along three rotational axis. This allows AEOs to further exhaust more imaging time of multiple targets which were previously assumed to be exclusive within the same time frame. This helps to maintain larger portions of the original schedule via an intricate suite of merging mechanisms to accommodate more acquisitions for each regular cycle of the scheduling horizon. In case sequences deemed less relevant than the incoming emergency request have to be deleted to free up availability or other resources, these get added to a backlog to be re-scheduled at a later point in time. Following a closely related approach with regards to merging sequences into existing schedules, Wang, Dai, and Vasile published an analysis on two heuristic scheduling algorithms in [41]. The two algorithms varied in their capabilities with regard to their allowed merging operations to alter the existing schedule. While the algorithm was allowed to either insert or delete with the option of later re-inserting based on a specific metric, the second heuristic method showed extended capabilities, including directly merging, shifting deleting, and re-inserting modifications. The authors were able to determine the first algorithm to be favorable in terms of run time and the second candidate to be superior with respect to overall algorithm performance.

### 3.3 Alternate Approaches

Optimization efforts for scheduling applications are self-evidently not limited to satellite operations. Widening the scope of this chapter beyond EO satellites, other types of spacecraft, such as rovers on different celestial bodies which do not have multiple ground station contacts every couple of hours, or deep space probes which need to be able to adjust their own operations automatically once they encounter anomalies in their nominal operations or any other application in which resources are allocated a priori with the goal of optimizing the returns based on the resources spent. This section is dedicated to offering an outlook beyond the intuitively similar cases to the underlying task of this thesis.

Commanding a spacecraft on another celestial body, in this case, the planet Mars, faces an utterly different environment. The formulation of mission goals and requirements needs to account for the latency e.g. when sending commands or receiving status updates, with no other means available to compensate for the inefficient use of mission time. In order to extract the maximum scientific return from a Mars rover mission, down-time of the spacecraft is the utmost unfavorable state. Insights presented by Sosland Siegfried et al. in [42] yield that the rover would enter a parking state and idle until new input from mission control arrives from Earth if any errors occur. Consequently, mission control of the Perseverance rover relies significantly on human judgement. Sequences have to be chosen carefully, often include sacrificing the chance of additional scientific return for the purpose of risk mitigation and minimizing idle time. The focus for the optimization of this scheduling problem was chosen to be on parallelizing efforts of rover activities. After extensive evaluation on ground, the team was able to develop a matrix illustrating the compatibilities of respective tasks being executed in parallel, following their fundamental notion of *thinking while driving*. The matrix assessed the compatibility and attributed each cell one of four designators to indicate whether parallelizing efforts are desired. Through executing tasks in parallel, not only is there a larger throughput of command sequences but it also allows MC on ground to operate with notably more up-to-date information, e.g. for cases where the environment of the rover was subject to change. The team of authors advised future missions to take parallelism into account already early in the design process of future missions in order to profit from this scheduling technique beginning with the first day of nominal operations.

The demonstrations presented so far focused on a centralized approach to the scheduling of one or multiple spacecrafts. This approach is attractive not only because it allows the involvement for human operators on ground if required but also as it transfers complexity from the space segment, the satellite, to ground. There, multiple iterations of hardware and software design can be performed if post-launch anomalies are encountered or improvements are identified. However, this sacrifices a certain amount of response time, as each command sequence depends on a previous ground station contact. However, this sacrifices a certain level of reaction time since each command sequence relies on a previous ground station contact. The way forward to mitigate this time lag when attempting to respond to rapidly changing environmental conditions that require adjustments to already planned sequences, for example, lies in the area of autonomous spacecraft operations. The motivation for autonomous spacecraft operations stems from applications that extend farther from Earth than conventional satellite orbits. Once the distances reach a certain magnitude, the delays in commanding due to physical limits of transmission speeds create impractical and potentially mission-critical delays. Hence, as explored by Rossi et al. in [43] for the exemplary case of a future mission evolving around robotic Solar System explorers, on-board autonomous scheduling of tasks is capable of providing the required performance with respect to achieving high-level scientific mission goals. The presented solution still relies on contact to ground but in contrast to the traditional approach of transmitting command sequences to the satellite the operators communicate their *intent* to the on-board scheduler. On-board scheduling allows an overall more opportunistic approach to the use of a spacecraft's resources.

At the same time, this technique allows significant improvements in the post-processing of sequences that have already been executed. On-orbit processing of the collected data will in turn reduce latency and overall response time to observations. Harris and Naik explored the potential of using a machine learning-based approach for autonomous scheduling of EO satellites in [44]. Using a Deep Reinforcement Learning (DRL) technique as an example, the authors compare their solution to state-of-the-art solutions that generally rely on approximations to propagate the spacecraft state. These approximations are by definition error-prone, which is traditionally resolved by sufficient margins or a higher level of accepted risk for infeasible schedules. An autonomous spacecraft, on the other hand, can react based on much more up-to-date information, allowing for better overall decision-making.

With this overview in mind, the next chapter dwells on the definition of the model architecture used within the scope of this work in order to solve the underlying optimization and scheduling problem. It shall demonstrate how certain aspects of the presented approaches can be customized to the specific task at hand based on the respective mission goals and requirements. With respect to this work, the general ap-

proaches for formulating the scheduling problem in a form that can be solved for constellations of satellites as well as the dynamic aspect of scheduling approaches find particular adaptation.



## 4 Model Architecture

This section introduces the model architecture behind the automated and optimized approach employed in the development of the OT-scheduling service. The term model should be interpreted as the formulation of the underlying problem into a mathematical description that can then be passed on to a solving algorithm. The expected in- and outputs are introduced first, before presenting the mathematical model description itself, including all parameters, constraints, and their respective interpretations. This derivation is built upon previous work, published in [26], that had been dedicated toward developing the automated scheduler for FOREST-1, OT's first satellite, and the lessons learned from that process.

The existing mission control infrastructure allows an automated creation of a schedule for FOREST-1, a single earth observation satellite operated as a hosted payload, with its focus set on optimizing toward complete resource allocation for bulk imaging over a list of targets. Consequently, with the timeline of OT's growing fleet of satellites, there is a clear need for incrementally expanding not only the grade of automation but also the capabilities of its mission operations. While it was sufficient for one member of the mission control personnel to execute one run of the scheduler for one specific satellite, one set of constraints regarding available on-orbit time and allocated data budget over a certain scheduling horizon, the approach to scheduling a constellation of satellites should be executed at regular intervals and have the capacity to treat the collection of satellites as one cohesive entity in order to maximize the added value by employing a dedicated constellation.

The imminent satellite missions at OroraTech will be operated as hosted payload missions. With this mission design, satellite bus operations are not required to consider when formulating the scheduling constraints, they can be assumed as given. Thus it is assumed that the technical boundary constraints imposed on the schedules of each satellite can be reduced to the following pair:

- The available power budget is interpreted as the amount of on-orbit time available for payload activities, evaluated per day.
- The data budget allocation is interpreted as the amount of data that can be generated and down-linked per day and limited over the same period.

Hosted payload missions help to reduce the complexity of the scheduling problem to mainly payload activity alone. Time slots reserved for housekeeping tasks, sun-pointing periods or ground station contacts are therefore interpreted as unavailable periods of on-orbit time. Hence, the projection of any type of sequence to on-orbit time stays viable even when moving from the simplified hosted payload case to operating all aspects of the spacecraft with the same scheduler. In principle, the model introduced in this section is designed to be transferable to any generic Earth observation satellite constellation which operates within a comparable framework. However, in order to take advantage from having access to two satellites that are currently in orbit and which can be interpreted as an exemplary constellation, the exact use cases and model parameters are chosen towards constituting the best fit to the OT satellite constellation. Therefore, standard mission operation tasks such as handling on-board housekeeping or scheduling downlink sequences are not included within the scope of this thesis. This is especially relevant since the following mission of building the first orbital plane filled with eight additional satellites will follow the same mission requirements while at the same time greatly increasing the complexity of solving the scheduling problem.

## 4.1 Use Case Analysis

The use cases of the scheduling component within the OT-scheduling service are depicted in Figure A.1.

The central use case in this application is clearly the automated and optimized scheduling of imaging payload activities across all available satellites. Firstly, there are two categories of imaging targets that need to be supported. There are areas of interest, e.g. customer areas, which shall be part of the selection of imaging targets usually throughout the entire lifetime of the mission as well as imaging requests which are expected but not limited to a specific target based on a pair of latitude and longitude coordinates. The respective imaging mode, whether to record both in the visible and infrared bands or infrared imaging only, shall be based on whether the respective satellite passes the target on ground during the day or not.

Furthermore, in addition to the listed imaging-targets there shall be an opportunistic operating mode that is dedicated to utilizing remaining resources via choosing additional imaging opportunities either over areas which are either expected to or do contain active wildfires. This for one results in a higher percentage of resource allocation towards payload activity but on the other hand helps to generate a larger body of thermal intelligence about ongoing fires.

While compiling automated schedules for each satellite within the constellation, each potentially available imaging opportunity shall be characterized by the following parameters:

- Category of imaging target (Area of Interest, Request, Opportunistic)
- Expected imaging conditions (Weather, Spacecraft orientation)
- Required resources to realize the respective opportunity.

Based on these parameters, the chosen optimization metric shall be designed to be able to decide between multiple possible imaging windows. This process shall then result in a set of conflict-free schedules which are tailored to achieving the largest possible contributions towards the mission goals.

Another crucial aspect of the design of the scheduling component within the OT-scheduling service is scalability with respect to the number of satellites within the constellation. The current timeline at OroraTech includes FOREST-2, another single satellite with a revised version of the imaging payload that has been tested and is still in operations on FOREST-1, which has been successfully launched in June of 2023. Moreover, the first orbital plane consisting of eight satellites, which are identical in design to FOREST-2, and FOREST-3, the first in-house developed satellite bus carrying the same camera, are scheduled to be launched within the next year. As the complexity of the scheduling problem can be expected to scale linearly with the number of satellites, as claimed by Eddy and Kochenderfer in [34], any model shall be designed with scalability in mind, especially in terms of algorithm selection and with that regarding computational and time effort necessary with every run of the scheduler. Therefore, the model shall support the addition of extra satellites, regardless of whether these are singular satellites or additional orbital planes, or whether they carry the same instruments or e.g. another revised version of the currently used imaging payload.

In addition to scalability, and especially concerning the mission operations of FOREST-3 and following missions, the design and implementation also have to be sufficiently flexible with respect to the manner of tasks in order to be able to keep up consistent schedules that exceed managing of payload activity alone. These might include handling housekeeping tasks onboard the satellite, active thermal control of the satellite and payload or including the necessary maneuvers and downlink sequences in each schedule. While this series of tasks has been excluded from the implementation related to this thesis, which will be presented in the following chapter, the baseline design shall at least include the necessary interfaces on which the desired capabilities can be built upon in the future nevertheless.

For the presented application, the reliability of the produced schedules is a major concern for mission control personnel as well as other stakeholders. Reliability in this context should be interpreted as the

certainty with which image acquisitions over high-priority targets within the predefined time spans are realized. The degree of necessary post-processing of collected infrared data and concerns about the time that passes between the imaging itself and the data having been fully downlinked to ground, what is usually referred to as latency, e.g. in [27], shall be neglected here. With the next satellites still being operated in a hosted payload manner, there is no direct influence of corresponding model parameters even if they were introduced at this stage of the development. The possibility to expand the model in such a way at a later stage shall be taken into account. However, the immediate way forward shall focus on how to guarantee the generation of conflict-free schedules which make full use of all assets that are part of the to-be-scheduled constellation. This could include, for example, merging multiple imaging sequences from the same satellite that would be scheduled in rapid succession without sufficient buffer time in between. Adequate buffer time between imaging windows would usually contribute to being protected against minor insecurities introduced by the higher number of attitude control maneuvers that might overlap with imaging activities. Therefore, the design of the scheduler shall include capabilities to mitigate too-tight scheduling by merging individual windows. With respect to the aforementioned flexibility in the model design, additional effort shall be spent on how and where to parallelize payload activities wherever applicable.

Further reliability assurances shall be achieved via a twofold approach. On one hand, schedule generation shall be performed in a timely manner with respect to the execution of the chosen sequences. With the earlier introduction of imaging conditions as part of the optimization metric, closing the time gap between prediction and conduction is especially relevant. The intended workflow of the scheduler is to be automatically executed at regular intervals in advance for a certain time span, the so-called scheduling horizon. This scheduling horizon should reach sufficiently further into the future than the next planned run of the scheduler. In doing so, each schedule that is uplinked and stored onboard one of the satellites covers against any issues that might occur during planned ground station contacts or the lack thereof. Therefore, the design of the scheduler shall include a sensible trade-off between the time between each schedule generation, the length of the scheduling horizon, and the number of schedules stored onboard each satellite in order to introduce the intended level of redundancy.

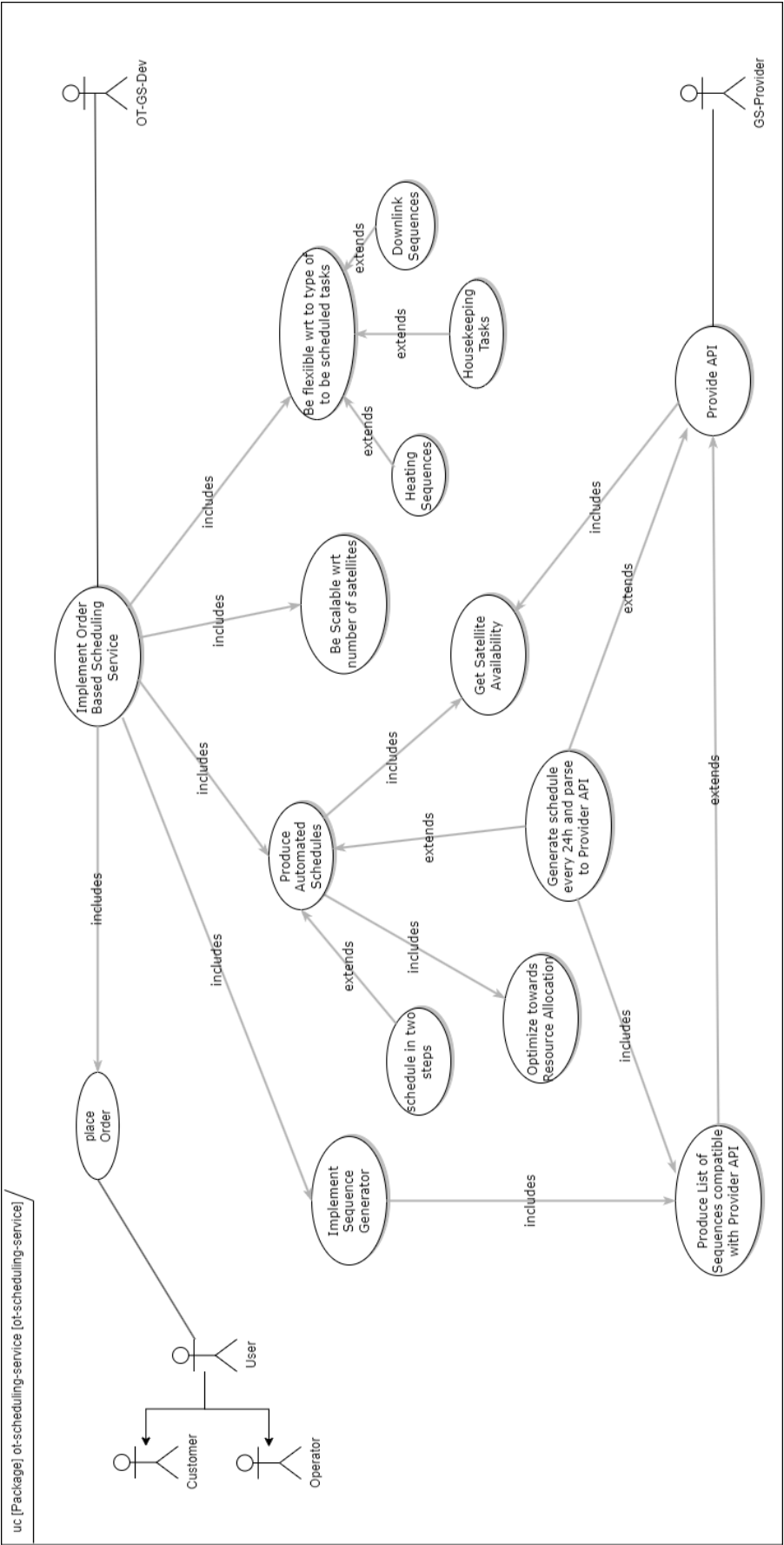


Figure 4.1 Diagram depicting the most important use cases stated at the beginning of this work.

From these previously formulated use cases, the following list of capabilities of the scheduler can be derived:

- Automatically generate new schedules in a timely manner with respect to the execution of the planned sequences.
- Manage and optimize towards resource allocation within the specified boundary constraints.
- Find matching epochs of upcoming overpasses over imaging targets.
- Gather predictions for expected imaging conditions.
- Offer a format to define areas of interest as well as imaging requests.
- Allow different levels of prioritization for specified set of targets.
- Implement an orbit propagator to predict the ground track of each satellite within the scope of the scheduling horizon.
- Find a scalable approach with respect to the size and shape of the constellation.
- Find a flexible approach with respect to the manner of tasks that exceed payload activities.
- Introduce reliability by sufficiently de-conflicting schedules via merging of too closely spaced imaging sequences.
- Introduce a certain level of redundancy via keeping more than one schedule in the onboard storage.

## 4.2 Model Description

This section introduces the mathematical model behind the optimization metric that has been employed to facilitate the selection of to be scheduled sequences based on the available set of imaging opportunities within the specified boundary constraints.

In general, any intersection between the propagated ground track of any satellite within the constellation with any target listed with the OT-scheduling service is defined as a so-called imaging opportunity. The model categorizes each of this number of  $i$  available imaging opportunities associated with a satellite  $j$  by the following set of parameters:

- Imaging Time  $t_{img,ij}$  [s],
- Amount of produced Data  $d_{win,ij}$  [MB],
- Figure of merit  $\eta_{fom,ij}$  [-].

It is worth mentioning at this point that the model itself is designed to be agnostic of ongoing wildfires. Instead, these occurrences are introduced into the model the same way any other targets enter the scheduler. While up-to-date information about ongoing fires is something the service shall also deliver, the main use case behind the WFS is to offer early detection of emerging fires with the lowest achievable latency. Thus, while a higher prioritization might be the intuitive approach it would on the other hand hinder early detection and is therefore overruled. Ongoing wildfires are covered via another set of imaging opportunities as part of the opportunistic operating mode.

While the values for the parameters for the to be allocated imaging time and amount of produced data are self-evident, the decisive element of the metric is the so-called figure of merit  $\eta_{fom,ij}$ . It is defined as follows:

$$\eta_{fom,ij} = p_{ij} \cdot (1 - c_{ij}) \cdot \cos(\varphi_{roll,ij}) \quad (4.1)$$

The influence of the roll angle  $\varphi_{roll,ij}$ , the required deviation from nadir-pointing to capture a specific target on ground, is modeled similarly to an angle of incidence on a solar panel by applying the cosine. The allowable roll angle is limited by the instrument-specific swath angle in both directions. These limits are deduced from the fact that adjacent ground tracks are designed to overlap with each other, such that any imaging opportunity outside of this range also exists with a smaller and therefore more desirable roll-angle with another satellite on the same orbital plane.

$$\varphi_{roll,ij} \in [-\varphi_{swath}, \varphi_{swath}] \quad (4.2)$$

In this case,  $c_{ij}$  denotes the expected percentage for cloud coverage, based on predictions requested at the time of schedule generation in combination with cached historic values of cloud coverage for the respective target:

$$c_{ij} \in [0, 1] \quad (4.3)$$

The term  $p_{ij}$  introduces a measure of priority assigned to each possible window and is calculated as follows:

$$p_{ij} = w_{type} \cdot w_{mode} \cdot p_{rel} \quad (4.4)$$

Default values are assigned depending on the type of window  $w_{type}$  which is either an area of interest or an imaging request, which are expected to be a single pair of coordinates related to a specific target. The exact values for these parameters need to be chosen with respect to the respective mission requirements and the expectations towards the behavior of the scheduler. OT's use case of providing thermal intelligence for the early detection of wildfires relies on generating coverage of the related areas of interest, which cannot be limited to a few specific targets.

$$w_{type} = \begin{cases} w_{aoi,default} & \text{for Area of Interest,} \\ w_{req,default} & \text{for Imaging Requests} \end{cases} \quad (4.5)$$

Equally, default values are assigned depending on the respective imaging mode  $w_{mode}$ . The mode denotes whether imaging is performed either both in the visible and infrared spectrum or in the infrared spectrum only. Ideally, imaging is performed using both spectres for a variety of reasons, e.g. training algorithms that rely on the availability of corresponding RGB frames.

$$w_{mode} = \begin{cases} w_{VIS\_IR,default} & \text{for VIS\_IR,} \\ w_{IR,default} & \text{for IR} \end{cases} \quad (4.6)$$

The term  $p_{rel}$  represents a measure for the relative priority assigned to the respective window by the user, which could be either a customer or mission control personnel. In contrast to the previously introduced priority term  $p_i$  which is used to establish an overall metric among all available windows, the relative term ranks an imaging target with respect to the other targets coming from the same source.

$$p_{rel} \in [0, 10] \quad (4.7)$$

Putting all of the above together, the target function behind the optimization metric can be fined as follows:

$$Z = \sum_i \sum_j (\eta_{fom,ij} \cdot t_{img,ij} \cdot x_{ij}) \quad (4.8)$$

where the term  $x_{ij}$  represents a decision variable.

This approach reduces the initial problem statement to accumulating as much return on figure of merit from choosing the right combinations of ideal imaging conditions and net imaging time within a given set of constraints imposed on each satellite individually. With that, the optimization problem for scheduling a number of  $j$  possible windows for  $i$  available satellites can be formulated as follows:

$$\text{maximize } Z = \sum_i \sum_j (\eta_{fom,ij} \cdot t_{img,ij} \cdot x_{ij}) \quad (4.9a)$$

$$\text{subject to } g_1(t_{win,ij}) = \sum_i \sum_j t_{win,ij} \leq t_{OT,max,i}, \quad (4.9b)$$

$$g_2(d_{win,ij}) = \sum_i \sum_j d_{win,ij} \leq d_{OT,max,i}, \quad (4.9c)$$

$$x_{ij} \in [0, 1] \quad (4.9d)$$

with the amount of spent time and aggregated data per window:

$$t_{win,ij} = t_{img,ij} + t_{oh,default} \quad (4.10)$$

$$d_{win,ij} = t_{img,ij} \cdot n_{fps,ij} \cdot d_{frame}(w_{mode,ij}) \quad (4.11)$$

This approach includes a necessary distinction between the actual imaging time per window per satellite  $t_{img,ij}$  and the overall time that has to be allocated in the schedule for the whole payload window  $t_{win,ij}$ .

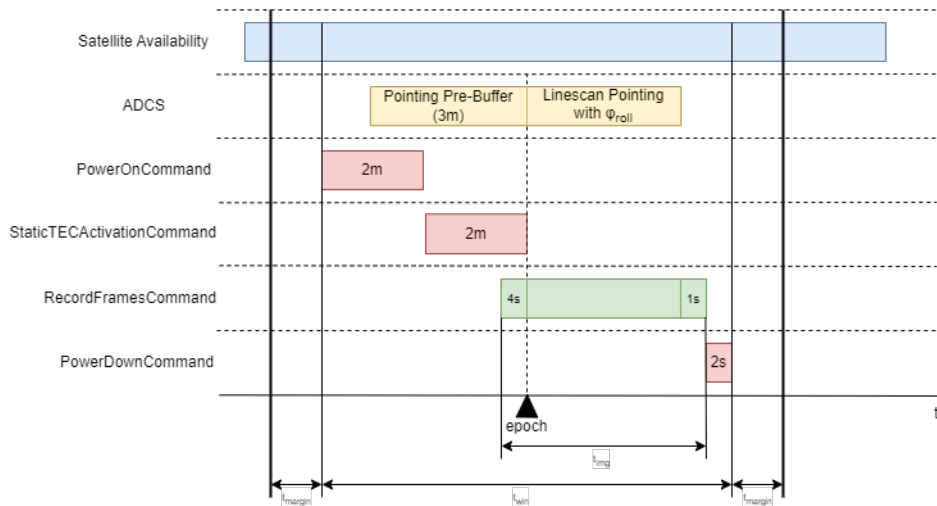


**Figure 4.2** Illustration how the different commands, execution times and margins constitute an imaging window and book a certain period of available on-orbit time of the satellite.

The latter term additionally accounts for the overhead connected with each imaging sequence, as illustrated in Figure 4.2. The actual start time for the imaging sequence, later referred to as the *epoch* of a window, is flanked by margins and buffers to account for the expected overhead. The overhead comes from the required Attitude Determination and Control System (ADCS) maneuver to align the satellite with the required roll angle, pre-heating of the instrument and some more time for on-orbit post-processing. Additionally, this overhead serves as a time buffer to mitigate the risk of too tightly packed schedules which might cause scheduled windows to fail due to unforeseen overlaps.

The amount of data which will be collected with each window is calculated via multiplying the net imaging time  $t_{img,ij}$  with the scheduled number of frames per second  $n_{fps,ij}$ , in order to obtain the number of recorded frames, and the amount of data per frame  $d_{frame}$ , which is a function of the respective imaging mode  $w_{mode,ij}$ .

As introduced earlier, the scheduling problem was in principle approached as a resource allocation problem. With this approach, the complexity has been successfully broken down to just two main constraints, the maximum of available on-orbit time for each satellite  $t_{OT,max,i}$  per day and the maximum amount of data than can be generated and downlinked per satellite within one day  $d_{OT,max,i}$ , as introduced in the equations 4.9b and 4.9c respectively. The presented approach does not employ any model for the on-board power storage. This is possible because the scheduling problem within the given scope at this point is limited to the scheduling of payload operations only. Thus, as long as the constraints for the payload duty cycles defined in the respective concept of operations are fulfilled, there a no power budget related issues to be expected. The satellite bus is expected to cut off the power supply to the payload in case power budget constraints were to be violated in a critical manner. This approach also forgoes modeling the on-board storage due to the sizing of the available storage in relation to the available downlink per day. Using FOREST-2 as the baseline for this assumption, the storage can accommodate the data from two full days of operations, e.g. in case there are no ground station contacts available for down-linking data from the satellite. While this case would be an exception from nominal operations, this margin also allows averaging the scheduling constraints over multiple days, opening more opportunities for maximizing the accumulated merit.

-

This chapter established the model architecture behind the scheduling approach that has been developed over the course of this work. With this, the next chapter will introduce and describe the steps taken during the implementation process of the described mathematical model into the ground segment environment currently in development at OT. The chapter will introduce the central components and their working principles on an architectural level.



## 5 OT-Scheduling-Service Implementation

The introduction of the OT-scheduling service is the logical next step in moving away from the manual mission operations that had been employed during the early operations of OT's in-orbit demonstrator mission FOREST-1 toward an automated approach to operating a growing fleet of satellites. Besides the immediate next satellite missions which will continue the hosted payload approach, current development efforts are oriented at delivering an in-house solution for the employed satellite platform. Combined with the plans for building up a large constellation of EO satellites in the near future, this not only calls for a scalable but also a flexible solution for the to-be-developed mission operations approach. The term scalability is to be understood as the capability to handle a larger number of, from a mission control perspective, identical satellites. Flexibility, on the other hand, is the ability to handle more advanced spacecraft tasks, such as scheduling housekeeping tasks or ground station contacts. Ultimately, flexibility requires a comprehensive scheduling solution.

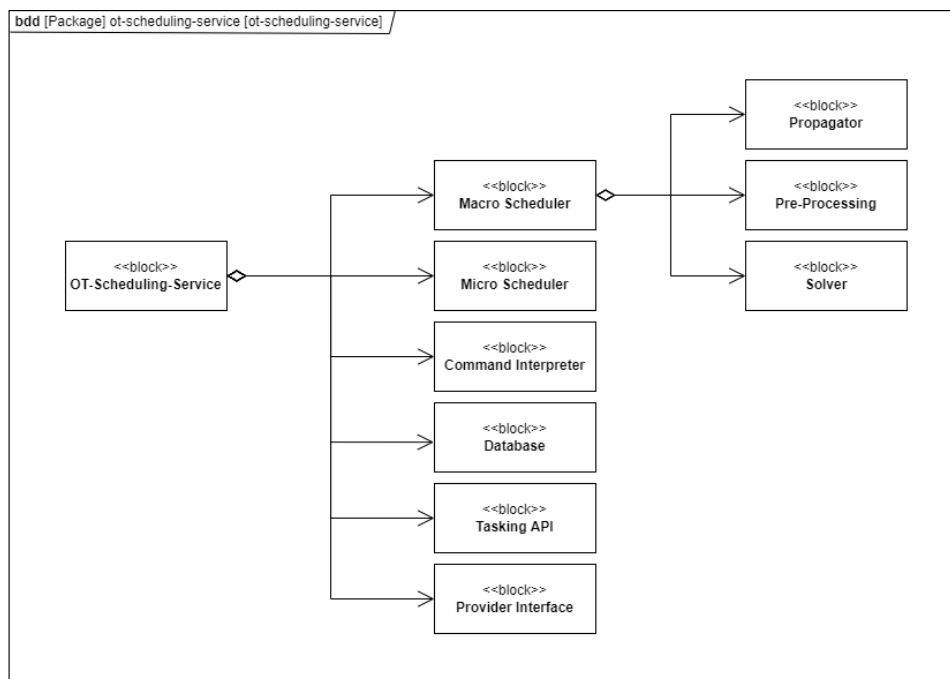


**Figure 5.1** Block definition diagram illustrating all implemented components of the OT-scheduling-service.

This section intends to present and put the implementation of the previously introduced methods into the context of the newly developed order-based scheduling service which is designed to be employed as the baseline concept of mission operations for any existing and future satellites launched by OroraTech. The required components of this service are listed in Figure 5.1, with a more in-depth description of the *Macro Scheduler* to follow in subsection 5.2.1.

## 5.1 Order Types

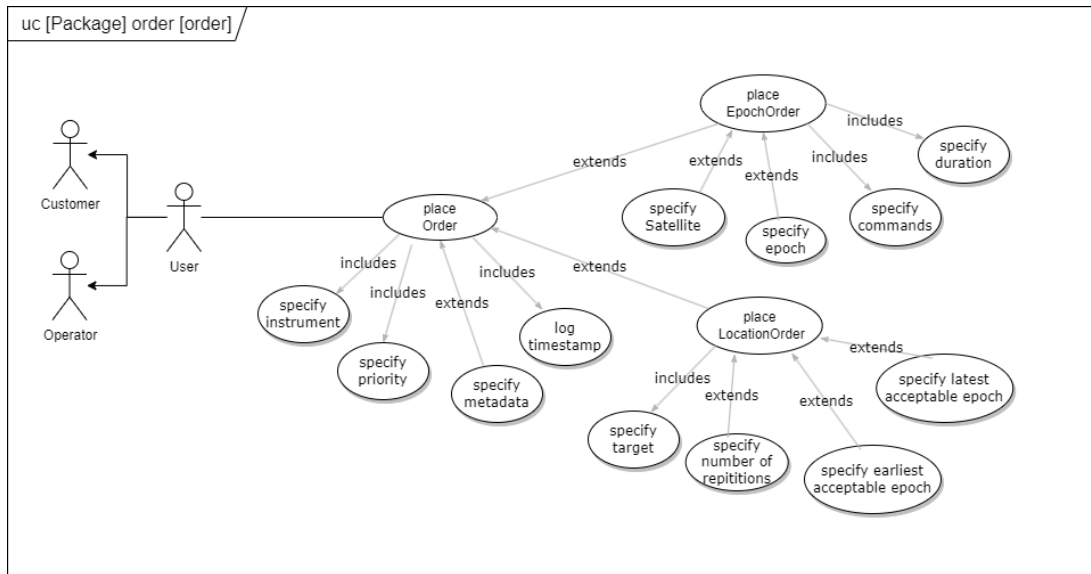


**Figure 5.2** Use Case diagram to illustrate the potential application types of both order types.

The approach that has been chosen for the future ground segment development at OT is oriented at an order-based, tasking-oriented scheduling platform. Thus, the prospected users shall be able to place an order with the OT-scheduling-service, which will then be automatically processed. As illustrated in Figure 5.2, the primary users of this service were identified to either be satellite operators in MC or customers directly. Both groups impose specific requirements. Two types of orders have been drafted to cover all expected use cases during satellite operations: the *LocationOrder* and the *EpochOrder*.

The underlying order type covers aspects that are relevant in both cases, such as the requested instrument on-board the spacecraft, an indication for the priority of an order, logging a timestamp at which the order was placed, or additionally any sort of metadata. Metadata can cover arbitrary information, e.g. a description of the requested sequence. For customers, the central use case evolves around placing a *LocationOrder* with the scheduling service. A *LocationOrder* is based on a request to image a specific target on Earth. Possible target formats are either a pair of coordinates or an area target, referred to as an Area of Interest (AOI) within the scope of this work. These are expected to come into the scheduling service either as imaging requests on short notice or in the form of permanent imaging targets, e.g. applicable for customer areas. Each order shall allow adjusting a period of time in which the imaging shall take place and the number of repetitions thereof, if desired. The imaging sequences themselves shall be standardized and follow default specifications, e.g. default values for the configured frame rate of the imaging instrument. Considering the scheduling context, the processing of a *LocationOrder* requires mapping an order onto one or multiple available satellite overpasses over the requested target on ground, thereby creating a relation between the imaging order and the set of spacecraft carrying the desired imaging instrument. When scheduling for a whole constellation of satellites, the expectation, in this case, would be numerous opportunities with multiple assets for the same order. Similarly, the imaging conditions of a target on ground are subject to change and might show significant variation, even for overpasses in quick succession of each other. Consequently, these circumstances allow for a high ceiling of optimization, especially with respect to the goal of optimal allocation of on-board resources for each spacecraft. Therefore, the collection of permanent and opportunistic imaging orders are parsed to the *Macro Scheduler*, which has been designed to optimize the highest achievable return of high-quality thermal-infrared data through an optimized utilization of available in-orbit satellite operations.

The *EpochOrder* was designed for more specific commanding of a specific spacecraft. In principle, each *EpochOrder* includes a set of commands intended for a specific satellite, at a specific time, called epoch,

which requires a certain duration to be executed completely. This opens a wide field of possible applications during satellite operations. These might include more complex imaging sequences, diverging from the default line-scan imaging mode with a fixed spacecraft orientation throughout the imaging window. Additionally, the *EpochOrder* allows the user to send command sequences for instrument calibration, maintenance, or software updates. Moreover, the interface can be used to transmit commissioning sequences during Launch and Early Orbit Phase (LEOP) of satellite newly added to the constellation. However, since each *EpochOrder* is bound to a specific epoch, therefore also to a specific satellite, there is no room for any kind of optimization efforts. Nevertheless, these orders still do have an impact on overall resource utilization. In order for the scheduling service to be not subjected to comparing two crucially different order types, *EpochOrders* are processed without triggering the automated imaging schedule generation. Instead, the scheduling service assesses whether the specified satellite is available at the requested period of time and adjusts the available resources for that particular asset of the constellation accordingly.

## 5.2 Scheduling Workflow

The overall workflow of the scheduling component within the OT-scheduling-service is depicted in Figure 5.3. Other components include the database in which pending and already processed orders are stored and logged, the orbit propagator which allows the user to calculate future overpasses of specific satellites and select based on this information, or external APIs, e.g. used for the prediction of the expected cloud coverage. The database is further used to store information about the state of the constellation, including the available satellites together with up-to-date TLEs and their operational state.

The scheduling service in itself is hosted on a Representational State Transfer (REST) API, modeled in Figure 5.3 as an *Idle* state. The service starts processing once a new order is placed by the user. Then, there are two distinct cases.

First, if the incoming order fits the format of an *EpochOrder*, the scheduling service issues an availability check of the specific satellite at the requested epoch for the respective duration. If the check fails, the order will be logged nevertheless and the user shall receive an error message indicating a scheduling conflict due to requesting an unavailable window. On the other hand, if the satellite is indeed available during the desired period, the *EpochOrder* is further parsed through the *Command Interpreter*. This component is responsible for translating the incoming *EpochOrder* format, designed to be easy-to-use on ground for human operators, into a command sequence that is executable on-board the satellite. Afterward, the assembled sequence is transmitted to the *Provider Interface*, usually another API hosted by the operator of the hosted payload satellite platform. This interface is responsible for uploading any generated satellite window or schedule from ground to the respective satellite in space. A sufficiently sized ground station network in order to reach each asset of the constellation in a timely manner is connected to the infrastructure behind the provided interface.

Second, for a new incoming *LocationOrder*, this order is processed through the two schedulers, the *Macro Scheduler*, whose workflow is described in more detail in subsection 5.2.1, and the *Micro Scheduler*. This process is not only triggered by an incoming imaging order, but is also executed periodically in order to ensure continuous operations and optimized imaging activity and resource utilization across the permanent targets. From a top-level view, the task of the *Macro Scheduler* is to predict and map the body of available upcoming imaging opportunities including the respective imaging conditions on ground onto the set of available and suitable satellites in order to generate the schedule of imaging activity. Refined by the collected metadata, the set of potential imaging opportunities is parsed to the solver component. The solver is set up to maximize the return on accumulated figure of merit  $\eta_{fom}$ , as introduced in Equation 4.9a, while optimizing towards optimal resource allocation. Allocated resources are subject to the pair of scheduling constraints introduced in section 4.2 for the maximum allowable in-orbit time for payload activity as well as the maximum available on-board storage. The resulting selection of to-be-scheduled imaging opportunities is then parsed onto the *Micro Scheduler*. At this point, each order has been assigned a specific epoch

and consequently a specific satellite. The *Micro Scheduler* translates this input into a set of the already discussed *EpochOrder*, in order to only use one common data class from there on. Therefore, the process afterward is identical to the case of handling an *EpochOrder*.

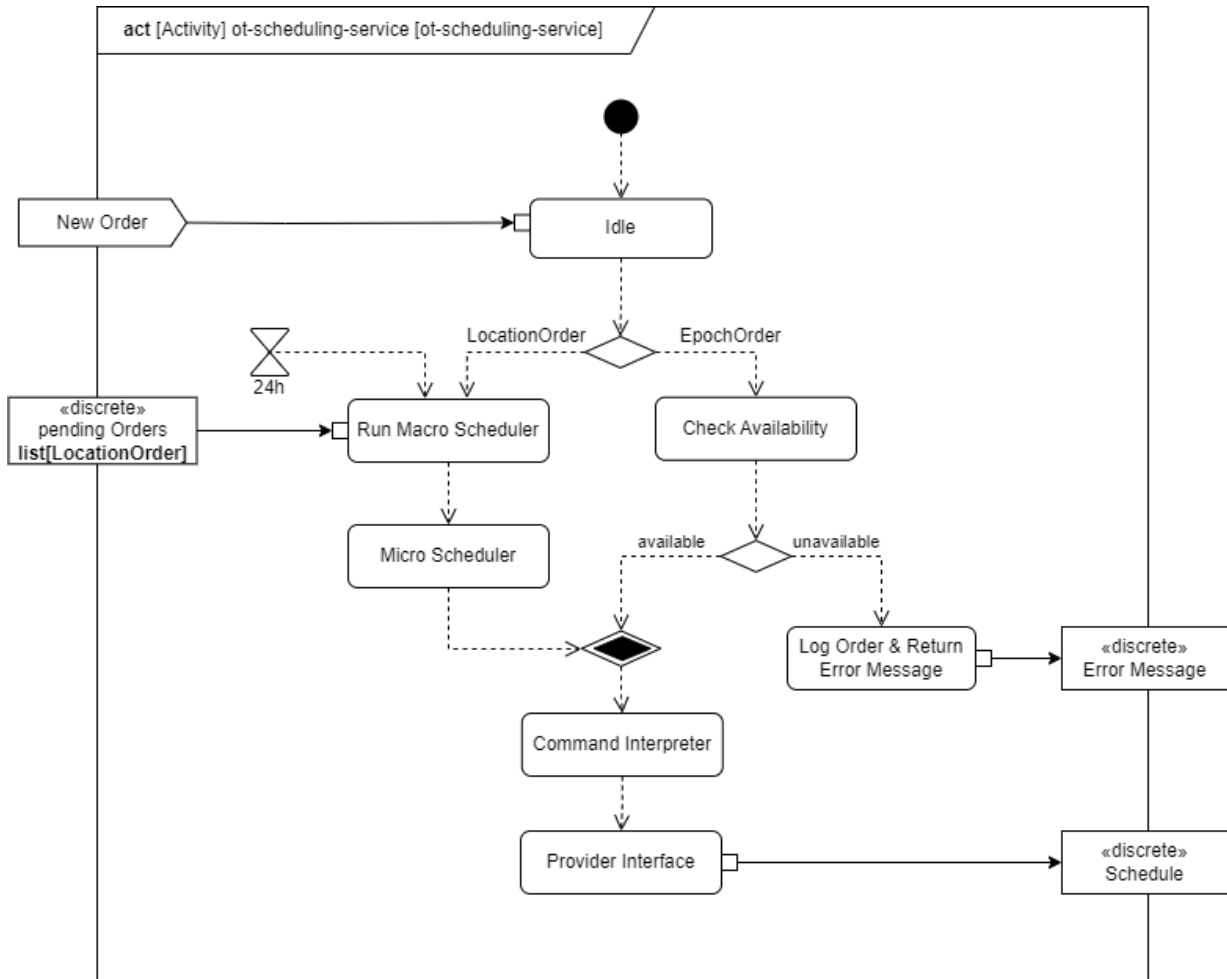
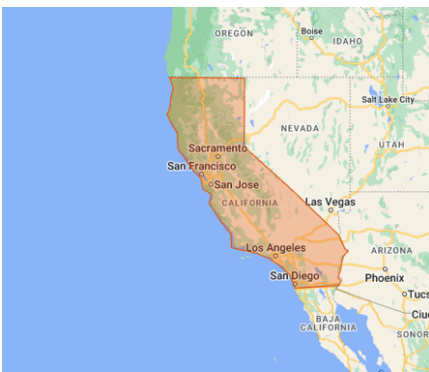


**Figure 5.3** Activity diagram illustrating the overall workflow of the OT-Scheduling Service for new incoming and pending orders and periodic automated schedule generation.

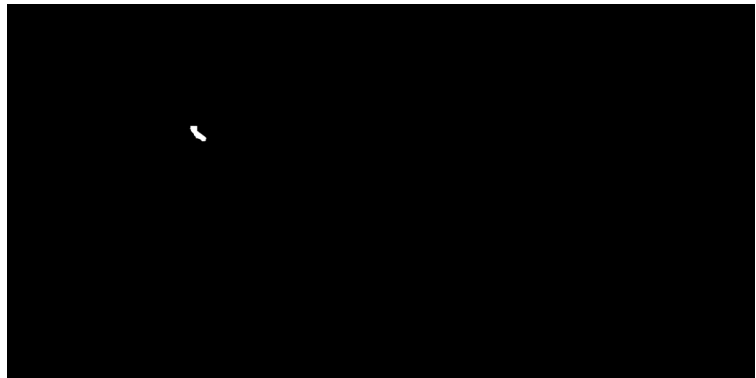
### 5.2.1 Macro Scheduler

The *Macro Scheduler* is the central component of the optimization effort in payload window scheduling for the OT satellite constellation. It incorporates the implementation of the scheduling approach introduced in section 4.2. Its nominal workflow for the automated and optimized scheduling of recurring targets is illustrated in Figure 5.5. This use case evolves around an existing list of pending *LocationOrders*, which enter the scheduling component from the underlying database. This list contains pending orders whose number of requested repetitions have not been fully fulfilled yet on top of the orders that represent permanent imaging targets.

In the first step, there is a check whether new targets have been added to the map containing the permanent targets. The map offers an easy-to-use and easily adjustable way for the respective operator to add, adjust or remove areas, specified by simple polygons. In general, the maintenance of this map falls to MC personnel, while other users are expected to issue imaging orders with targets based on a pair of latitude and longitude coordinates. In case there are changes in the existing map of AOI targets, the scheduler executes an update loop. In the first step, these polygons, each representing one AOI, are partitioned into individual files. Each polygon is reduced to a white polygon and projected onto black ground, maintaining its position with respect to its coordinates on an isometric projection. This transformation for the exemplary AOI representing the state of California is illustrated in Figure 5.4, with the polygon on top of a regular map in Figure 5.4a and the resulting projection for the same area on the right in Figure 5.4b.



(a) Polygon framing the state of California as an AOI target.



(b) [Projection of the polygon representing the state of California as an AOI file.

**Figure 5.4** Comparison between the two stages of importing an AOI target into the set of permanent imaging targets of the *Macro Scheduler*.

Once an up-to-date set of permanent imaging targets has been evaluated, the *Macro Scheduler* proceeds by using the propagator built into the OT-scheduling-service to calculate every upcoming overpass for each imaging order within the specified scheduling horizon. The propagator yields the epoch for the point at which a predicted ground track crosses the boundary of an AOI, the corresponding necessary roll angle  $\phi_{roll}$  to capture a target, and the duration of the available overpass. The preprocessing required to prepare the solver input further involves gathering information about expected cloud coverage via a call to a corresponding external API. The imaging mode  $w_{mode}$  of each imaging opportunity is determined via evaluating whether the target on ground is passed during daylight based on the respective epoch in the respective time zone. Imaging in both the infrared and visible bands is used for daylight overpasses, infrared imaging alone for nighttime overpasses. RGB imaging without daylight is considered as non-beneficial for the overall mission and is therefore avoided in order to optimize data budget allocation.

The next step involves an availability check for each satellite. As stated earlier, there are more tasks required for the commanding of a satellite such as housekeeping tasks or ground station contacts. These are scheduled outside of the optimized payload activity scheduler and therefore block certain periods of availability which consequently are not eligible for imaging windows. Imaging opportunities that would overlap with already scheduled satellite windows are therefore disregarded in the subsequent steps. This validates that there are no scheduling conflicts with already scheduled windows, regardless of the decisions made by the solver.

Then, the remaining set of imaging opportunities are entered into the solver component. In order to fit with the model architecture, that has been introduced in section 4.2, the available set of data needs to be formulated in the corresponding matrix notation. The proposed model foresees that each row in the matrices represents an imaging order, and each column represents a satellite. Thus, any entry in one cell of the matrix represents one specific imaging opportunity for one order with a specific satellite. This process is carried out for one matrix containing the corresponding imaging opportunities, and one matrix each with the values for the figure of merit  $\eta_{fom,ij}$ , window duration  $t_{win,ij}$  and the expected amount of acquired data  $d_{win,ij}$ . In case there are multiple imaging opportunities available for the same imaging order for the same satellite, only the opportunity with the highest values for the potential figure of merit  $\eta_{fom,ij}$  is used further. The other three matrices follow accordingly. The format of this matrix notation is shown in Table 5.1 for the exemplary case of a set of eight satellites within the same orbital plane for sixteen imaging orders. Subsequently, the result of the solver follows the same notation. The entries in the result, the assignment matrix, are either ones or zeros, corresponding to an imaging opportunity being selected to be scheduled in full, or not scheduled at all. Before passing on the result to the next step, the assignment matrix is mapped onto the matrix containing the imaging opportunities. The remaining result then consists solely of the to-be-scheduled entries.

Before parsing the resulting schedule to the *Micro Scheduler*, the output is examined for potential scheduling conflicts within the resulting schedule. Potential conflicts might stem from two sequences which might not have an overlap during their net imaging time  $t_{img}$  but still lack sufficient buffer before and after the imaging sequence itself in order to be approved. Windows that are sufficiently close together and compatible with respect to roll angle  $\varphi_{roll}$  and expected cloud coverage  $c$  are merged into one imaging sequence. Non-resolvable scheduling conflicts result in the omission of the sequence with the lower value for the respective figure of merit  $\eta_{fom}$ . This further ensures that only validated schedules are posted as a result of the scheduling component.

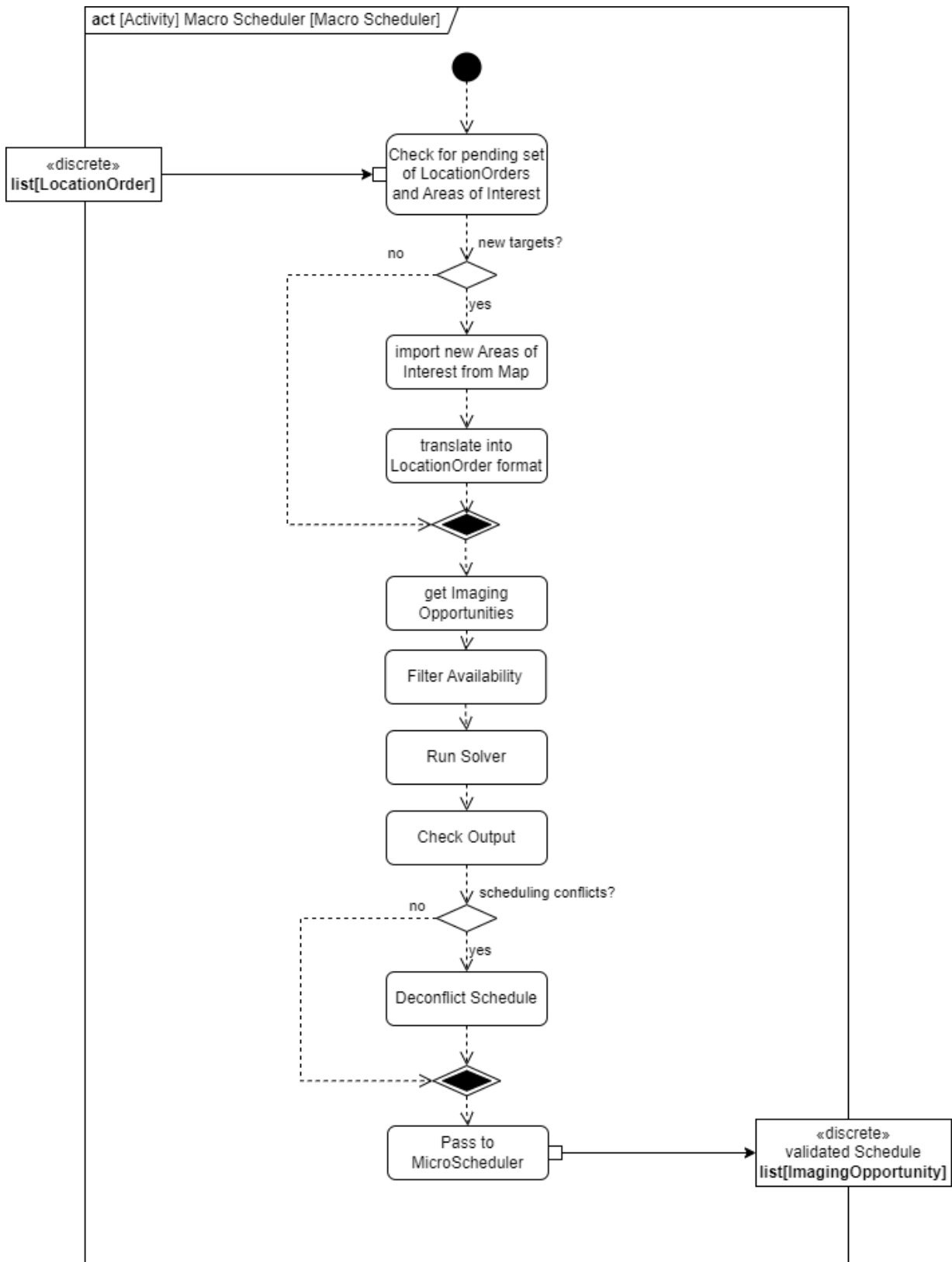


**Figure 5.5** Activity diagram illustrating the overall workflow of the OT-Scheduling Service for new incoming and pending orders and periodic automated schedule generation.

**Table 5.1** Table illustrating the matrix notation in which imaging opportunities are stored.

FOREST-1	FOREST-2	FOREST-3	FOREST-4	FOREST-5	FOREST-6	FOREST-7	FOREST-8
ImagingOpportunity(...)	ImagingOpportunity(...)	0	0	ImagingOpportunity(...)	ImagingOpportunity(...)	0	0
0	0	0	0	0	0	0	0
ImagingOpportunity(...)	ImagingOpportunity(...)	0	0	ImagingOpportunity(...)	ImagingOpportunity(...)	0	ImagingOpportunity(...)
ImagingOpportunity(...)	ImagingOpportunity(...)	ImagingOpportunity(...)	ImagingOpportunity(...)	ImagingOpportunity(...)	0	ImagingOpportunity(...)	ImagingOpportunity(...)
0	0	0	0	0	ImagingOpportunity(...)	0	0
ImagingOpportunity(...)	0	0	ImagingOpportunity(...)	ImagingOpportunity(...)	ImagingOpportunity(...)	ImagingOpportunity(...)	ImagingOpportunity(...)
ImagingOpportunity(...)	ImagingOpportunity(...)	ImagingOpportunity(...)	ImagingOpportunity(...)	ImagingOpportunity(...)	ImagingOpportunity(...)	0	ImagingOpportunity(...)
0	ImagingOpportunity(...)	ImagingOpportunity(...)	ImagingOpportunity(...)	0	0	0	0
0	ImagingOpportunity(...)	ImagingOpportunity(...)	ImagingOpportunity(...)	ImagingOpportunity(...)	ImagingOpportunity(...)	0	0
0	0	0	0	0	0	0	ImagingOpportunity(...)
0	0	0	0	0	0	0	0
0	0	0	0	0	0	0	0
ImagingOpportunity(...)	ImagingOpportunity(...)	0	0	ImagingOpportunity(...)	ImagingOpportunity(...)	0	0



### 5.2.2 Solver

The *Solver* component within the *Macro Scheduler* is tasked with solving the posed optimization problem. Hence, the choice of algorithm can have a significant impact on the quality of the produced results. More in-depth analysis and comparisons of applicable algorithms for solving a satellite constellation scheduling problem are presented by Sundar et al. in [45] and Globus et al. in [46]. For this particular use case, the two main requirements for the used solving algorithm have been to be applicable to solving MILP problems and to allow the matrix notation described in subsection 5.2.1. Moreover, compatibility with Python was required. The compatibility with MILP problems is justified by the fact that the formulation of the underlying problem of this work, specified in Equation 4.9a, is consistent with the overwhelming majority of scheduling approaches found and presented in chapter 3. Furthermore, since the scheduling constraints are formulated for each satellite individually, there was considerable justification for the matrix notation purposely designed for this use case.

In the end, the MILP solver, which is based on the open source linear programming package Python Linear Programming (PuLP), was chosen as the solving algorithm for the implementation of the OT scheduling service. From its documentation published in [47], the working principle can be understood as a platform which makes calls to industry-grade solvers such as CPLEX or the Computational Infrastructure for Operations Research (COIN-OR) Linear Programming Solver, whose detailed documentation can be found in [48] and [49] respectively. The chosen solver allowed for easy integration with the existing set of MC tools and the mode architecture introduced earlier in this thesis. Moreover, due to the extensive range of available interfaces to different solvers, which are automatically tried with each run of the solver, the chosen approach has exclusively shown stable behavior, remarkably short computation times in the order of magnitude of seconds, and convergence to an optimal solution throughout the development process of the approach to solving the satellite constellation scheduling problem presented here.

With this chapter, the steps that were taken during in order to translate the model architecture into a concrete application for the optimized scheduling of a satellite constellation have been introduced. For this purpose, the working principle of the *Macro Scheduler* as the central component with regard to the optimization of the schedule has been thoroughly illustrated. The design choices made during the development process, such as the format to be used for managing a large set of areas of interest or the choices regarding the *Solver* component, were also presented and discussed. Therefore, the following chapter will showcase the results for multiple scheduling scenarios that could be obtained with this implementation of a scheduling service and were used to validate the design decisions over the course of this work.

## 6 Scheduling Results

This section presents an overview of the scheduling results obtained over the development and research process behind this thesis. For this purpose, several constellation designs have been run through the scheduling process in order to determine how changes in size and shape affect overall constellation performance.

The results of the implemented scheduling approach shall be evaluated with respect to the respective resource allocation of on-orbit time as well as on-board storage. Further, the order fulfillment and the average number of repetitions per imaging order shall be compared as well. An order is considered fulfilled if at least one satellite within the constellation is assigned an overpass for the respective target. This shall suffice as a measure for the capabilities of a certain constellation design to service imaging requests in a timely manner. The four constellation designs presented range from two single satellites on two separate planes, to one, two, and four planes of eight equally spaced satellites each. In the latter cases, the orbital planes are also identically spaced.

The test case setup is identical for each scenario, with a scheduling horizon of two days, and the same set of AOI imaging targets. For each scenario, the resulting resource allocation of on-orbit time and on-board storage is illustrated below with a comprehensive comparison of all scenarios at the end of this section.

### 6.1 OroraTech Constellation

At this point in time, the OT constellation consists of two operational satellites in orbit, FOREST-1 and FOREST-2. This small constellation shall serve as the baseline scheduling scenario. From here, constellation performance is expected to increase significantly once the constellation is expanded by additional satellites and orbital planes.

The two satellites are each in two separate orbital planes, with the larger difference in RAAN at around  $159^\circ$ . With this setup, the two satellites were able to achieve an overall order fulfillment rate of 41.1%, with each order executed 0.47 out of a maximum of two times. The exact allocations for each satellite are depicted in Figure 6.1 and Figure 6.2, with an average allocation of 10.5% for on-orbit time and 74.5% for on-board storage.

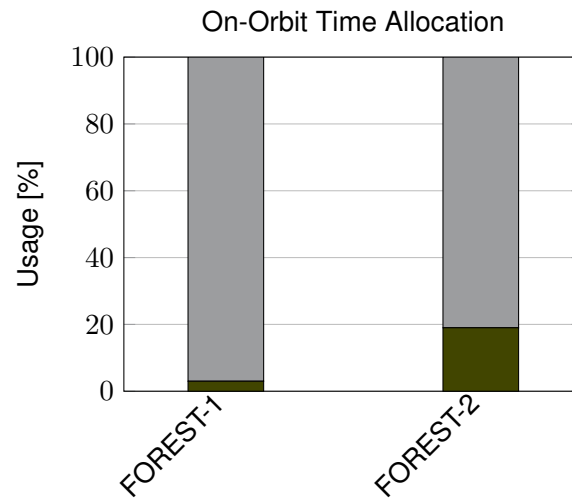


**Figure 6.1** Results for on-orbit time allocation from the scheduling result for the current OT constellation.

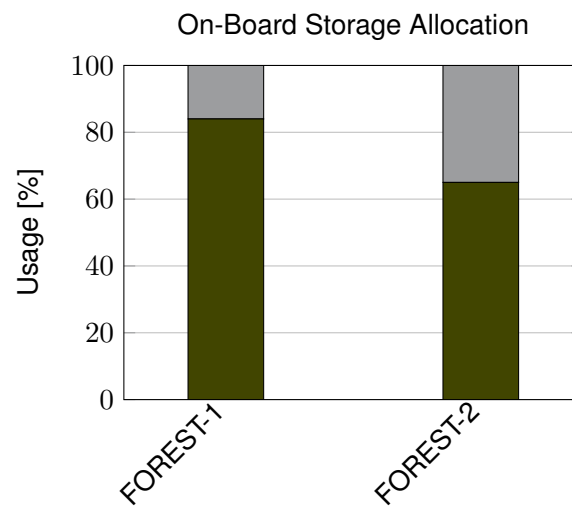


**Figure 6.2** Results for on-board storage allocation from the scheduling result for the current OT constellation.

## 6.2 One Orbital Plane

The first scenario that shall be evaluated represents the transition from single satellites on separate orbital planes to a constellation of eight satellites equally spaced within the same plane. With this, as introduced in chapter 2, a coverage overlap is ensured for all subsequent overpasses. Therefore, the optimization is expected to achieve a high fulfillment rate since there should be no targets missed by the constellation, assuming the target on ground is reachable within the specified scheduling horizon.

With the first orbital plane, the constellation was able to achieve an overall order fulfillment rate of 63.0%, with each order executed 1.70 out of a maximum of five times. The scheduled allocations for each satellite are depicted in Figure 6.3 and Figure 6.4, with an average allocation of 34.4% for on-orbit time and 98.9% for on-board storage.

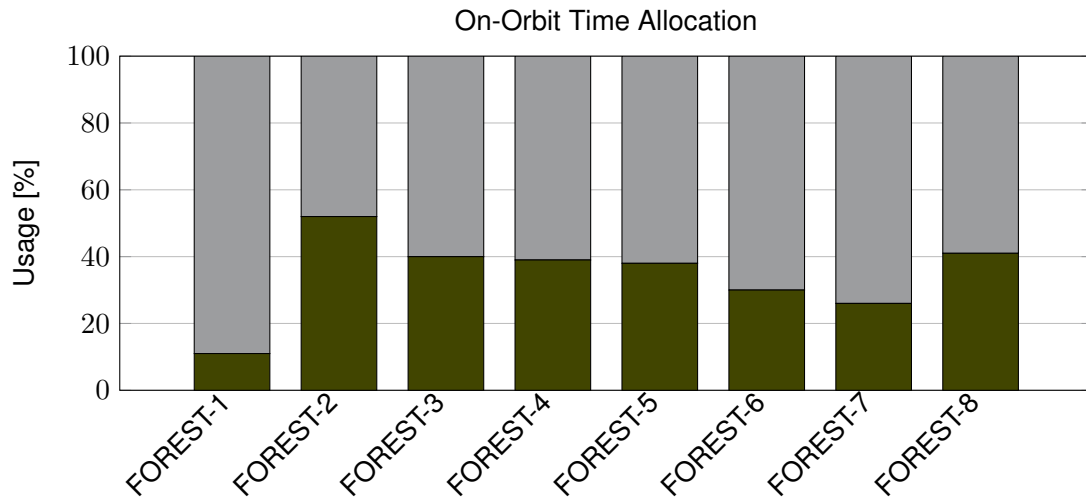


**Figure 6.3** Results for on-orbit time allocation from the scheduling result for the scheduling scenario of one orbital plane with eight satellites.

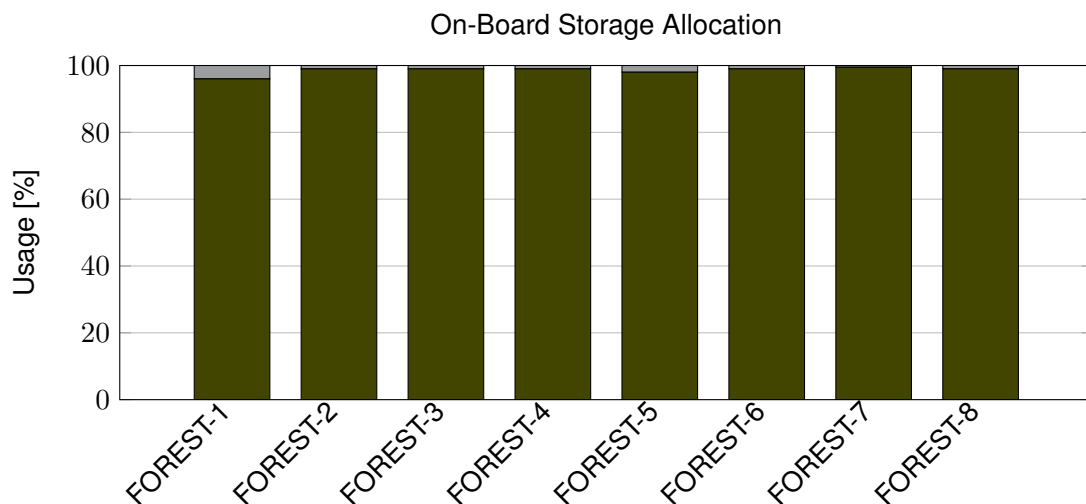


**Figure 6.4** Results for on-board storage allocation from the scheduling result for the scheduling scenario of one orbital plane with eight satellites.

### 6.3 Two Orbital Planes

Following the insights gained from the investigation into basic principles of constellation design presented in chapter 2, the next scenario was chosen to feature two orbital planes, with a RAAN shift of  $90^\circ$  and eight equally spaced satellite in each plane. Therefore, revisit time is expected to improve significantly, as the improvement from moving from one to two orbital planes has been observed in Figure 2.7 to be the largest step with respect to revisit time improvement, and with that the number of imaging opportunities for each processed order.

With this setup, the sixteen satellites were able to achieve an overall order fulfillment rate of 85.2%, with each order executed 3.1 out of a maximum of five times. Figure 6.5 and Figure 6.6 show the resource allocations for each satellite, with an average allocation of 32.0% for on-orbit time and 99.0% for on-board storage.

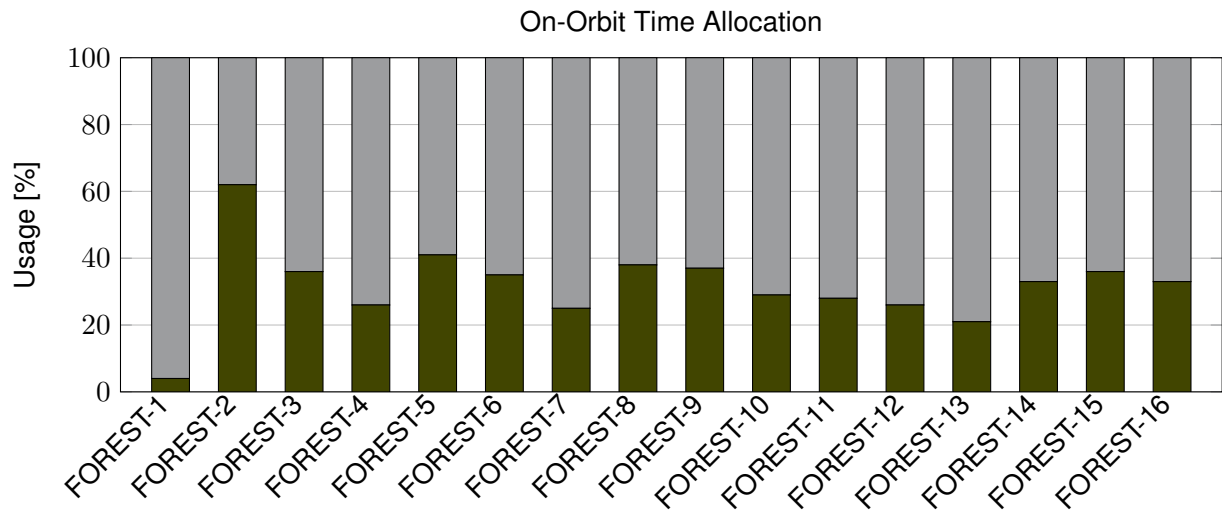


**Figure 6.5** Results for on-orbit time allocation from the scheduling result for the scheduling scenario of two orbital planes with a difference in RAAN of  $90^\circ$  with eight satellites each.

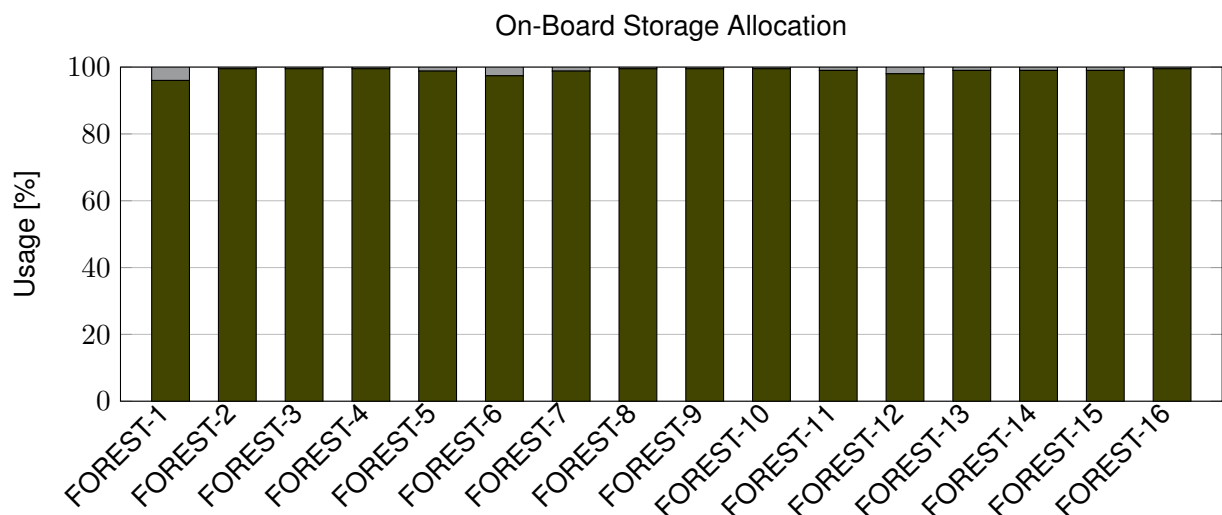


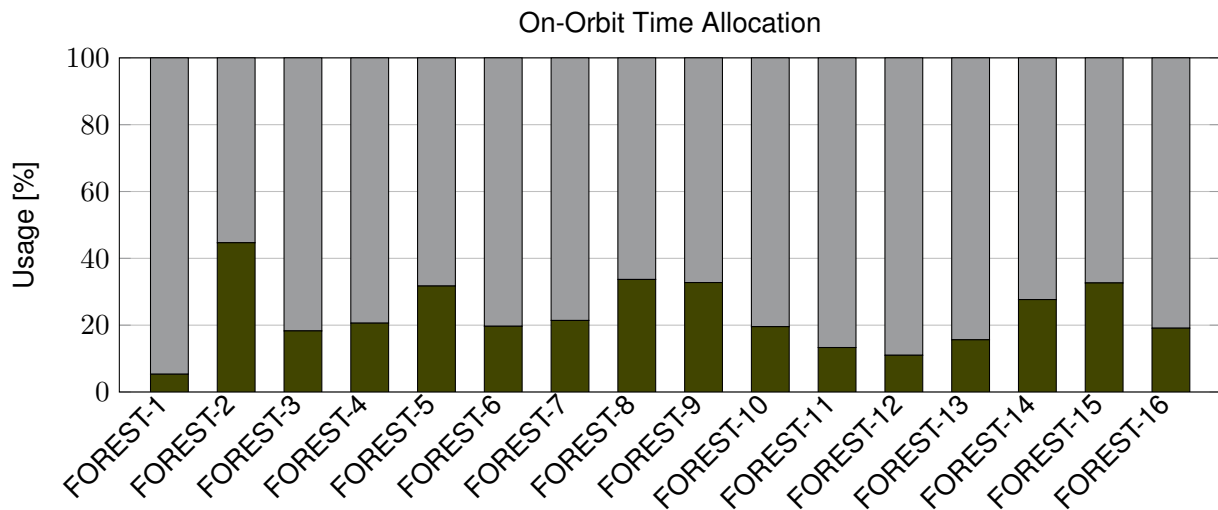
**Figure 6.6** Results for on-board storage allocation from the scheduling result for the scheduling scenario of two orbital planes with a difference in RAAN of  $90^\circ$  with eight satellites each.

## 6.4 Four Orbital Planes

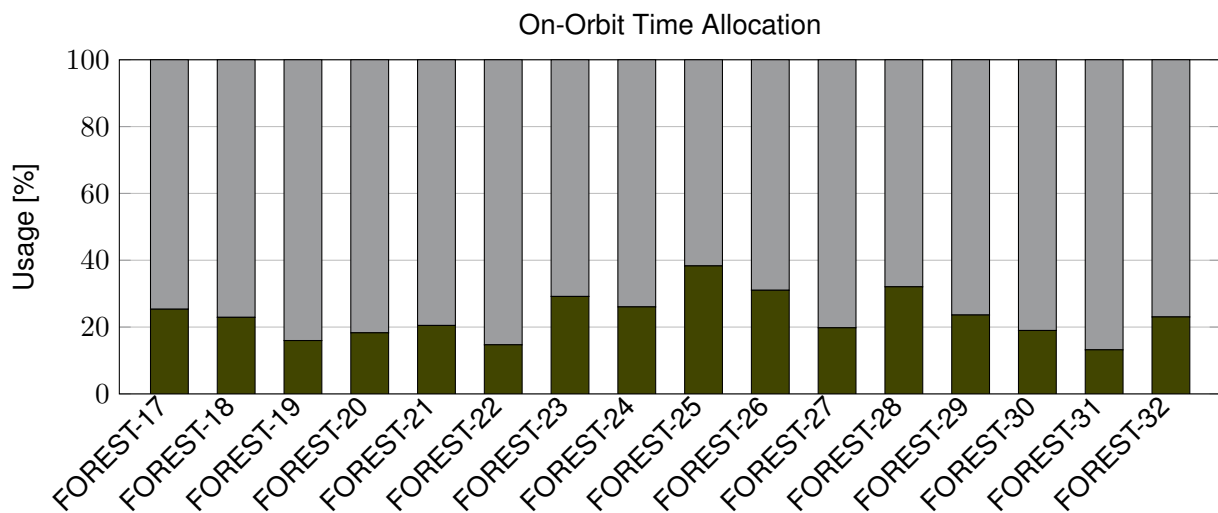
Finally, this test case features four orbital planes, with a RAAN shift of  $45^\circ$ , and again eight equally spaced satellites in each plane. This again follows the approach for expanding a satellite constellation that has been presented in Figure 2.7. The expectation for this scenario is another reduction in revisit time and therefore a higher number of imaging opportunities, but a smaller increase than the one observed for the step between one and two planes. With the higher number of imaging opportunities, order fulfillment rate should also increase.

This constellation design featuring thirty-two satellites was able to achieve an overall order fulfillment rate of 96.3%, with each order executed 4.5 out of a maximum of five times. Figure 6.5 and Figure 6.6 show the resource allocations for each satellite, with an average allocation of 23.1% for on-orbit time and 98.6% for on-board storage.



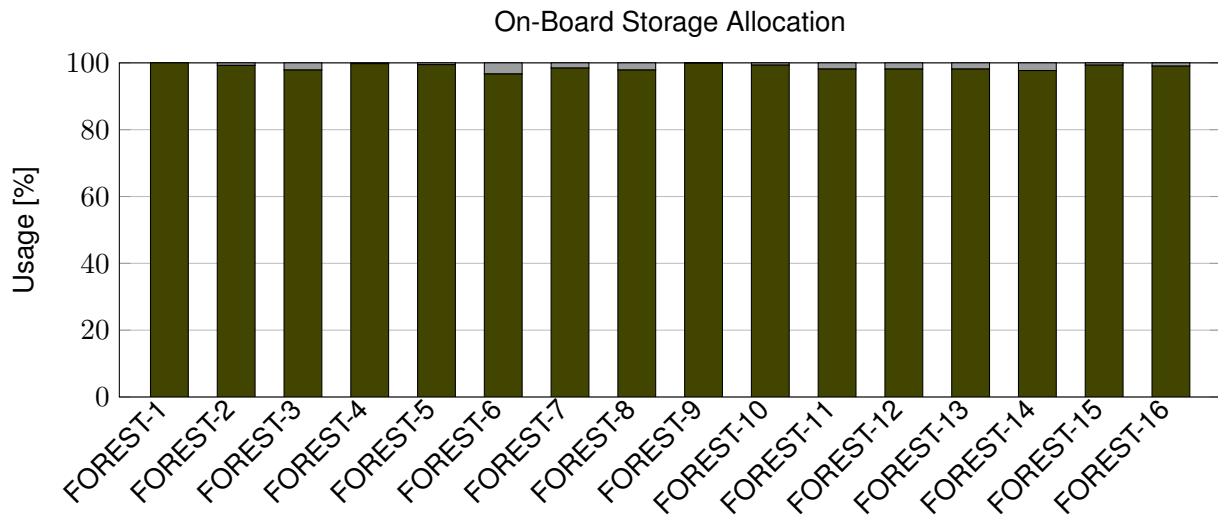


(a) Results for FOREST-1 through FOREST-16.

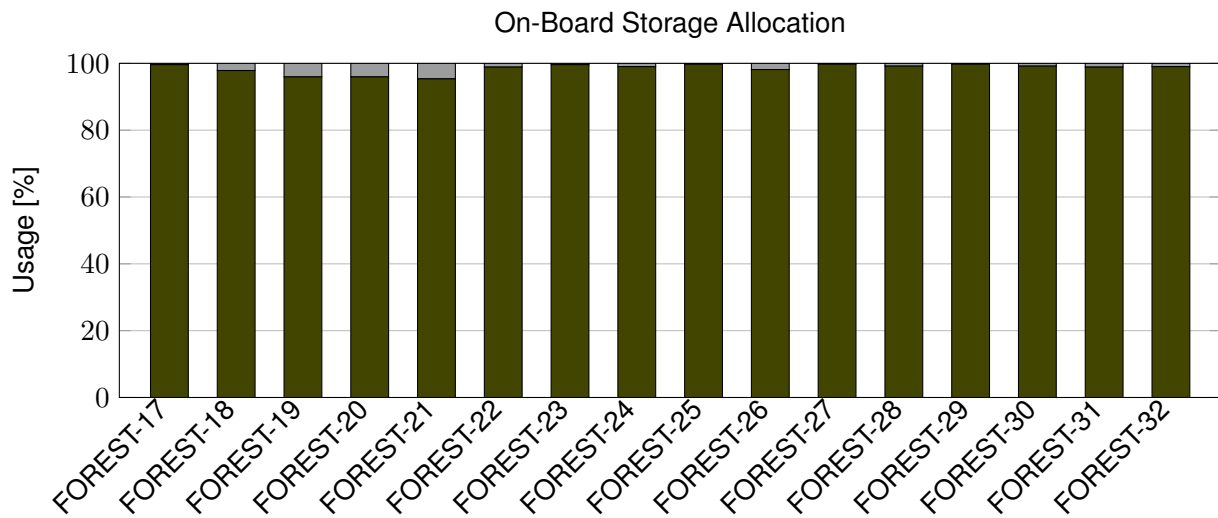


(b) Results for FOREST-17 through FOREST-32.

**Figure 6.7** Results for on-orbit time allocation from the scheduling result for the scheduling scenario of four orbital planes with a difference in RAAN of  $45^\circ$  with eight satellites each.



(a) Results for FOREST-1 through FOREST-16.



(b) Results for FOREST-17 through FOREST-32.

**Figure 6.8** Results for on-board storage allocation from the scheduling result for the scheduling scenario of four orbital planes with a difference in RAAN of  $45^\circ$  with eight satellites each.

## 6.5 Random Constellation Design

In order to demonstrate the effect of purposely designed constellations, this scenario consists of eighteen EO satellites in LEO. Hence, there is a similar number of total satellites to the example presented in section 6.3, but for this case all satellites are orbiting on their own randomly spaced plane. Therefore, there is no coherent recognizable constellation design pattern to be found. Instead, constellations like this example might be chosen for use cases where operators do not possess the capabilities to launch a dedicated EO constellation and have to rely on data from already existing satellites. While it is unlikely for such a use case to employ a centralized scheduling approach, it shall be used as an example in this case nevertheless.

With this setup, the two satellites were able to achieve an overall order fulfillment rate of only 48.1%, with each order executed 0.39 out of a maximum of five times.

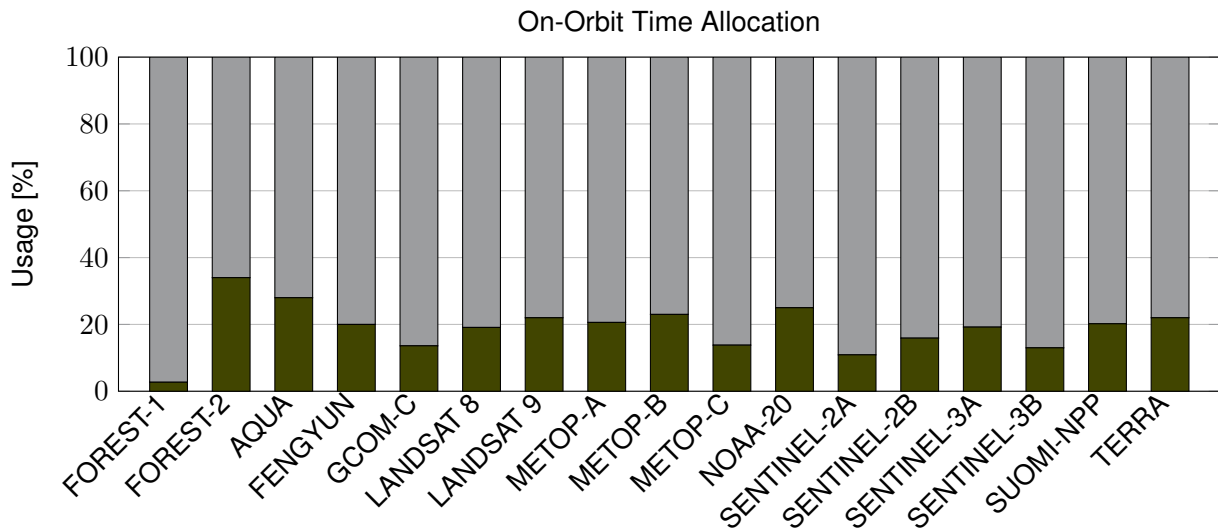


**Figure 6.9** Results for on-orbit time allocation from the scheduling result for the scheduling scenario of eighteen satellites with each on its own orbital plane with the set of planes randomly spaced between them.

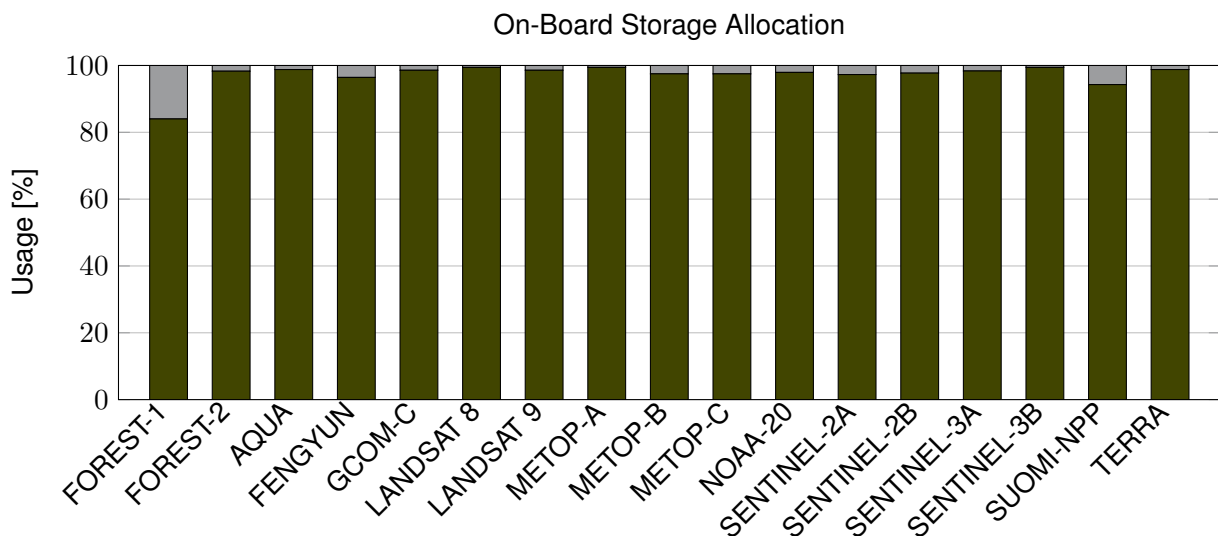


**Figure 6.10** Results for on-board storage allocation from the scheduling result for the scheduling scenario of eighteen satellites with each on its own orbital plane with the set of planes randomly spaced between them.

## 6.6 Comparison

Comparing all of the results obtained over multiple constellation design scenarios offers multiple insights into the behavior of the approach presented in this thesis. Table 6.1 lists the produced results for the five test cases that have been introduced within this chapter and compares them with respect to their average values for resource allocation and the achieved order fulfillment rate in percent. Overall, multiple runs of the *Solver* for the same input of available imaging opportunities have yielded equal results for each execution.

In every one of the observed test cases, the availability of on-orbit time has shown to be of no particular concern, even less so for larger constellations with more available satellites to fulfill the collection of imaging orders presented to the scheduler. Instead, the available on-board storage could be identified as the constraining factor for this problem. The only case where the allocation does not come close to reaching the upper boundary is for the two-satellite test case. This can be traced back to the considerably lower number of available overpasses, and therefore lower number of imaging opportunities in general to fulfill the provided orders. However, once the number of available imaging opportunities exceeds the availability of the on-board storage resource, the scheduling problem becomes *over-booked*. Then, instead of being able to plainly assign the, according to the employed model for the *figure of merit*, best available imaging opportunity in each case, the solver shows to select the final schedule with the objective of resource optimization.

It is remarkable that for the two scenarios of two purposely designed orbital planes with eight satellites each and the eighteen randomly arranged orbits, the order fulfillment rate has been observed to be noticeably worse for the random constellation design. Even though both scenarios feature a comparable number of total satellites, following the two examples for possible constellation design guidelines presented within this work help to extract more potential in the form of a 15% improvement of overall order fulfillment rate.

**Table 6.1** Comparison in scheduling results for the presented scenarios.

Scenario	No.Sats	No.Planes	Avg. On-Orbit Time %	Avg. On-Board Storage %	Order Ful. %
Two Sats	2	2	10.5%	74.5%	41.1%
One Plane	8	1	34.4%	98.9%	63.0%
Two Planes	16	2	32.0%	99.0%	85.2%
Four Planes	32	4	23.1.0%	98.6.0%	96.3%
Random Const.	18	18	19.0%	97.2%	48.1%

## 7 Conclusion

This section presents the conclusions that can be drawn from the results that were obtained from the research and development efforts within the scope of this thesis. Further, these results shall be put into perspective based on the respective expectations for their behavior with respect to changes in the size and shape of an EO satellite constellation.

The contributions of this thesis are two-fold. First, the findings and conclusions from the presented study of the characteristics of constellation performance parameters are discussed. Secondly, the automated scheduling solution that has been implemented and tested within the scope of this thesis shall be presented and further evaluated with respect to how adjustments in the theoretical limits of satellite scheduling based on the underlying constellation design are mirrored in the scheduling output. Both aspects shall complement each other in answering the central research question of this thesis.

Regarding the design of a future constellation, the fundamental principle of designing toward a specific set of mission goals and requirements stands. For the particular category of EO satellite constellations, the presented steps of establishing an overlap between subsequent satellite footprints first and to then start to add additional orbital planes, each with a sufficient number of satellites, present a solid baseline in the process of defining a preliminary constellation design.

The number of satellites per orbital plane has been identified as a crucial design decision for an incremental construction of a satellite constellation. In order to minimize cost and complexity each launched collection of satellites shall be sized in such a way as to account for the minimum number of satellites required per orbital plane to achieve continuous coverage through a coverage overlap of subsequent satellites. Once this overlap has been achieved, additional measures can and should be considered to account for individual satellites undergoing maintenance or dropping out of the constellation completely. However, for an initial design, the minimum number plus one spare satellite shall be considered as sufficient for a minimum viable solution.

Once continuous coverage is ensured, the addition of more orbital planes to the constellation has been identified as the central design parameter to be leveraged in order to reduce the maximum revisit time for the respective set of targets on Earth. Maximum revisit time was chosen as the critical performance parameter for any EO activity that benefits from low latency, most prominently disaster management and response use cases such as the early detection of wildfires targeted by OT. The effect of adding more satellites to the same number of orbital planes has been shown to be the negligible effect compared to increasing the number of planes. Both the effect of increasing the number of satellites within an orbital plane and the effect of increasing the total number of orbital planes show a tendency to respond quickly in the beginning and eventually converge to a plateau. In the case of coverage overlap, the achieved overlap converges asymptotically to the swath width on ground. This is an indication to further pursue different constellation patterns or designs which are purposely designed to service specific regions on Earth in case these basic principles do not achieve to break through these performance plateaus.

Furthermore, regarding the implications for the scheduling of an EO satellite constellation, a successful implementation of an order-based scheduling architecture based on the model presented in this work has been achieved. The implementation encompasses two distinct forms of accepted order types which are capable of handling any sort of required tasks required to operate a satellite constellation in LEO.

The results indicate that the problem becomes overbooked as soon as the number of available imaging opportunities and their associated costs exceed the available resources with respect to the scheduling

constraints. Before that, e.g. in the case of two single satellites, the scheduling problem reduces to simply assigning the best opportunity for each order since the number of available overpasses within the scheduling horizon does not reach the constraints. From the results obtained for the resource allocation in the presented test cases, the scheduler shows a clear tendency towards two aspects. First, the solver achieves convergence to what can be considered as a complete allocation of the available on-board storage, without exceeding the scheduling constraints in any observed test run. Second, it shows that the on-board storage represents the far more restricting constraint with its maximal allocation at only 34.4%. These observations were made for the specific example of multiple scheduling scenarios within the constraints that were imposed on the OT constellation and are not necessarily transferable to other environments without corresponding adjustments. However, the goal of maximizing resource utilization within a hosted payload context for a satellite mission stands. In addition to this, some imaging orders could not be fulfilled within the given two-day planning horizon for any of the constellation designs presented. With the expected cloud coverage exerting a crucial influence on the figure of merit, and therefore the allocation of resources towards an imaging opportunity, consistently unfavorable imaging conditions for certain regions on Earth might offer an explanation for the lack of consideration. However, convergence could be observed for each tested scheduling scenario. Therefore, the scalability of the presented scheduling approach has been demonstrated.

The observation regarding the upper limit for on-board storage being identified as the far more constraining factor opens the discussion about adjustments in the overall mission Concept of Operations (ConOps). In particular, exploring the possibilities of adding more ground station contacts or optimizing the on-board data handling opens up opportunities to increase the overall performance of the constellation. Significant potential could be identified to provide more resources to expand the amount of imaging activity and thereby achieve a significant increase in the return on figure of merit.

## 8 Outlook

In this section, possible directions for future developments of this approach and future work with respect to the OT-scheduling-service, in general, are briefly introduced. In addition, it touches on the aspects of this approach that have been acknowledged but were or could not be pursued further within the scope of this thesis.

In general, the direction in which OroraTech (OT) is moving at this point in time is toward expanding the number of satellites in orbit to incrementally improve the monitoring capabilities of their thermal-infrared EO satellite constellation. This path involves on one hand the adaption of a first dedicated orbital plane with eight more satellites based on the hosted-payload design as it has been used for the FOREST-2 mission and on the other hand the ongoing development of an in-house solution for the satellite bus. With launches for the first orbital plane with eight satellites and the first in-house mission FOREST-3 scheduled before the end of 2024, as announced in [50] and [2] respectively, it is imperative to scale the capabilities of the corresponding mission operations approach accordingly. This will introduce an increasing degree of heterogeneity to OT's satellite constellation. Thus, the OT-scheduling-service will need to be expanded accordingly. While, as concluded earlier, the scalability of this approach has been proven over the course of this thesis, the flexibility to handle both hosted-payload and in-house developed satellite bus based assets within the same constellation will be a major challenge in the foreseeable future.

The flexibility of the presented scheduling approach could not be proven with a meaningful test case within the scope of this work. Nevertheless, the introduced approach to formulating the optimization problem offers every required capability to be transferred to e.g. the scheduling of a single satellite with multiple to-be-scheduled payloads on-board. The only component that would need to be adapted is the pre-processing unit within the scheduler, which in its current state collects all the scheduling metadata, e.g., the expected cloud coverage, epochs of available overpasses, and so on.

Still, the payload scheduling presented in this approach does lack some key features for it to be a complete solution for every sort of tasking which is required during the whole mission lifetime of a satellite. Desirable improvements include scheduling of ground station contacts, automated commissioning of newly launched satellites that are to be added to the existing constellation, or periodic maintenance and calibration sequences. Since all of these categories of operations tasks exhibit recurring patterns, there remains significant potential for further automation of the overall scheduling process. Especially with the projected growth of the constellation, maximizing the grade of automation becomes increasingly desirable in order to most effectively use human resources on ground as well as on-board resources in space.

Moreover, as already briefly touched on in section 3.3, potential candidates for future developments might lie in the field of on-board scheduling. This would shift the paradigm from centralized management of all aspects of satellite operations from a coherent ground segment to a decentralized approach on board each spacecraft. This selection of spacecrafts would in turn have to be able to communicate with each other such that this scheduling approach does not neglect the potential of scheduling as a constellation over the handling individual satellites on their own. Current advancements in Artificial Intelligence (AI) research hold significant promise for providing a complementary set of tools to the current approaches in order to further improve the efficiency and performance of future EO satellite constellations.



# A Appendix

# A.1 Full Use Case Analysis

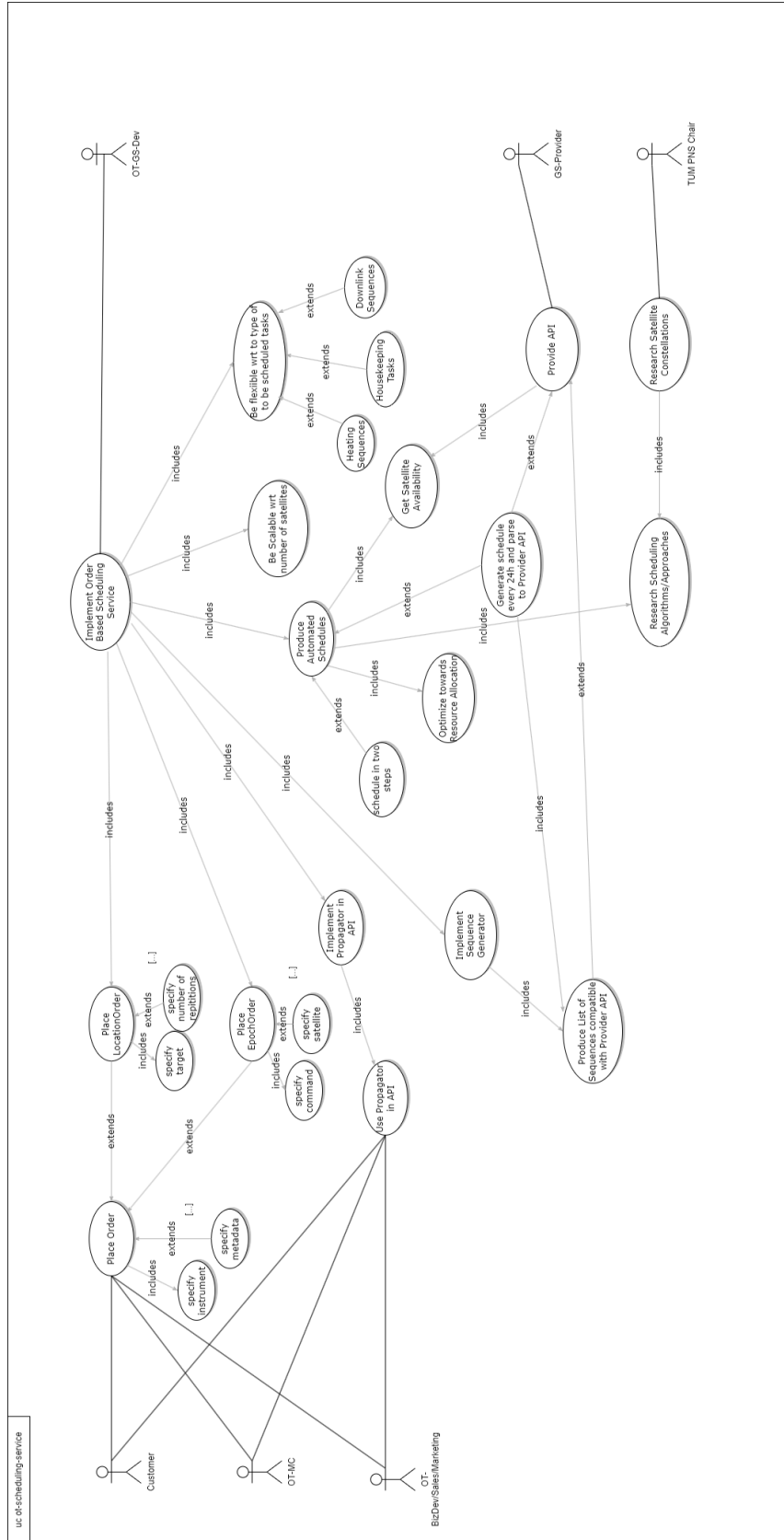


Figure A.1 WIP Update this with a diagram that shows only the discussed use cases which are actually related to the scheduler component/ Description of graphic.

## Bibliography

- [1] OroraTech. Maintain control of wildfires: Ororatech launches global thermal intelligence service. <https://ororatech.com/ororatech-launches-global-thermal-intelligence-service/>, 2023. Accessed: 25 July 2023.
- [2] OroraTech. Ororatech accelerates deployment of its multipurpose thermal satellite constellation. <https://ororatech.com/ororatech-accelerates-deployment-of-its-multipurpose-thermal-satellite-constellation/>, 2022. Accessed: 25 July 2023.
- [3] J. Indrikis and R. Cleave. "SPACE EGGS" - Satellite Coverage Model for Low Earth Orbit Constellations. 1991.
- [4] Walker, J.G. Satellite Constellations. *Journal of the British Interplanetary Society*, 37:559, December 1984.
- [5] J.G. Walker. Continuous whole-earth coverage by circular-orbit satellite patterns. *Royal Aircraft Establishment*, 1977.
- [6] D. Mortari, M.P. Wilkins, and C. Bruccoleri. The flower constellations visualization and analysis tool. *The Journal of the Astronautical Sciences*, 52:107–127, 2004.
- [7] Ansys, Inc. Ansys stk. <https://www.ansys.com/products/missions/ansys-stk>, 2023. Accessed: 30 June 2023.
- [8] C. Bruccoleri and D. Mortari. The flower constellations visualization and analysis tool. In *2005 IEEE Aerospace Conference*, pages 601–606, 2005.
- [9] M.E. Avendaño, J.J. Davis, and Mortari D. The 2-d lattice theory of flower constellations. *Celestial Mechanics and Dynamical Astronomy*, 116:325–337, 2013.
- [10] D. Arnas, M. Lifson, R. Linares, and M.E. Avendaño. Definition of low earth orbit slotting architectures using 2d lattice flower constellations. *Advances in Space Research*, 67, 2020.
- [11] U. Walter. *Astronautics: The Physics of Space Flight*. Springer Cham, 3 edition, 2019.
- [12] SpaceX. Smallsat rideshare program. <https://www.spacex.com/rideshare/>. Accessed: 24 June 2023.
- [13] ICEYE. New benchmark in imaging from sar microsattellites: Iceye presents 25 cm azimuth resolution. <https://www.iceye.com/blog/new-benchmark-in-imaging-from-sar-microsatellites-iceye-presents-25-cm-azimuth-resolution>, 2023. Accessed: 24 June 2023.
- [14] S. B. Shah, T. Grübler, L. Krempel, S. Ernst, F. Mauracher, and S. Contractor. Real-Time Wildfire Detection from Space - a Trade-Off Between Sensor Quality, Physical Limitations and Payload Size. *ISPRS - International Archives of the Photogrammetry, Remote Sensing and Spatial Information Sciences*, 4216:209–213, September 2019.

- [15] Spacenews. SpaceX launches eighth dedicated smallsat rideshare mission. <https://spacenews.com/spacex-launches-eighth-dedicated-smallsat-rideshare-mission/>, 2023. Accessed: 08 July 2023.
- [16] Wiley J. Larson and James R. Wertz. *Space Mission Analysis and Design*. Third edition, 1999.
- [17] T.N. Assmann. Design and optimization of a cubesat constellation for wildfire detection, 2019.
- [18] P.G. Buzzi, D. Selva, N. Hitomi, and W.J. Blackwell. Assessment of constellation designs for earth observation: Application to the TROPICS mission. *Acta Astronautica*, 161:166–182, August 2019.
- [19] Y. Liu, Z. Wan, Y. Dai, Y. Zhao, Q. Liu, and C. Ji. Emergency constellation design based on micro sar satellites. In *2021 Global Reliability and Prognostics and Health Management (PHM-Nanjing)*, pages 1–5, 2021.
- [20] G. Zheng, Y. Yao, D. He, and H. Diao. Optimization design of global low-orbit satellite constellation for multi-fold coverage. In *2020 IEEE 3rd International Conference on Electronics and Communication Engineering (ICECE)*, pages 1–5, 2020.
- [21] Kongsberg Satellite Services KSAT. Global ground station network. <https://www.ksat.no/ground-network-services/the-ksat-global-ground-station-network/#>. Accessed: 15 July 2023.
- [22] A. Golkar. Architecting federated satellite systems for successful commercial implementation. In *AIAA SPACE 2013 Conference and Exposition*. AIAA SPACE Forum, 2013.
- [23] I. Sanad and D.G. Michelson. A framework for heterogeneous satellite constellation design for rapid response earth observations. In *2019 IEEE Aerospace Conference*, pages 1–10, 2019.
- [24] Official U.S. government information about the Global Positioning System (GPS) and related topics. Gps.gov. <https://www.gps.gov/systems/gps/space/>. Accessed: 15 July 2023.
- [25] European Space Agency. Building and testing spacecraft. [https://www.esa.int/Science\\_Exploration/Space\\_Science/Building\\_and\\_testing\\_spacecraft](https://www.esa.int/Science_Exploration/Space_Science/Building_and_testing_spacecraft). Accessed: 15 July 2023.
- [26] F. Strasser, M. Favin–Lévêque, T. Assmann, and F. Schummer. Algorithmic resource allocation for spacecraft operations. In *2023 IEEE Aerospace Conference*, pages 1–16, 2023.
- [27] J. Cappaert and et al. Constellation modeling, performance prediction, and operations management for the spire constellation. In *Proceedings of the 35th Annual Small Satellite Conference*, 2021.
- [28] V. Mallik, J. Mueting, A. Reuter, A. Paul, B. McGill, L. and Jagatia, and V. Shah. An automated approach to maneuver campaign management for skysats. In *Proceedings of the 36th Annual Small Satellite Conference*, 2022.
- [29] Planet Labs. High-resolution imagery with planet satellite tasking. <https://www.planet.com/products/hi-res-monitoring/>. Accessed: 16 July 2023.
- [30] S. Augenstein, A. Estanislao, E. Guere, and S. Blaes. Optimal scheduling of a constellation of earth-imaging satellites, for maximal data throughput and efficient human management. *ICAPS*, 26(1):345–352, 2016.
- [31] R. Nallapu, B. Jagatia, P. Linden, L. M. Donahue, and A. Ayasse. On-orbit demonstrations of proactive tasking of glint imagery. In *2023 IEEE Aerospace Conference*, pages 1–11, 2023.
- [32] Nicola Bianchesi and Giovanni Righini. A mathematical programming algorithm for planning and scheduling an earth observing sar constellation. 2006.

- [33] D. Cho, J. Kim, and J. Choi, H.and Ahn. Optimization-based scheduling method for agile earth-observing satellite constellation. *Journal of Aerospace Information Systems*, 15(11), 2018.
- [34] D. Eddy and M.J. Kochenderfer. A maximum independent set method for scheduling earth observing satellite constellations, 2020.
- [35] T. Arvidson, S. Goward, J. Gasch, and D. Williams. Landsat-7 long-term acquisition plan: Development and validation. *Photogrammetric Engineering Remote Sensing*, 72(10):1137–1146, 2006.
- [36] J.C. Pemberton and L.G. Greenwald. On the need for dynamic scheduling for imaging satellites. In *FIEOS*. ISPRS, 2002.
- [37] D. Liao and Y. Yang. Imaging order scheduling of an earth observation satellite. *IEEE Transactions on Systems, Man, and Cybernetics, Part C (Applications and Reviews)*, 37(5):794–802, 2007.
- [38] R. Medina, J. Redfern, and Z. Talpas. The punch mission planning system; the next iteration in micro-satellite constellation operations. In *2023 IEEE Aerospace Conference*, pages 1–8, 2023.
- [39] W.A. Fisher and E. Herz. A flexible architecture for creating scheduling algorithms as used in stk scheduler. 2013.
- [40] H. Sun, W. Xia, Wangm Z., and X. Hu. Agile earth observation satellite scheduling algorithm for emergency tasks based on multiple strategies. *J. Syst. Sci. Syst. Eng.*, 30(5):626–646, 2021.
- [41] M. Wang, G. Dai, and M. Vasile. Heuristic scheduling algorithm oriented dynamic tasks for imaging satellites. *Mathematical Problems in Engineering*, 2014, 2014.
- [42] R. Siegfriedt Sosland, A. Girerd, J. Hazelrig, D. Gaines, E. Fosse, A. Appakonam, N. Waldram, A. Plave, and M. Rozek. Enabling parallel activities for mars 2020 rover surface operations. In *2023 IEEE Aerospace Conference*, pages 1–18, 2023.
- [43] F. Rossi, D.A. Allard, R. Amini, T.S. Vaquero, N.N. Dhamani, V. Choukroun, M.and Verma, M. Jorristma, S. Davidoff, E.and Jasour A.and Hofstadter M. Francis, R.and Van Wyk, B.W. Huffman, A.C. Barrett, M.D. Ingham, and R. Castano. Workflows. user interfaces, and algorithms for operations of autonomous spacecraft. In *2023 IEEE Aerospace Conference*, pages 1–17, 2023.
- [44] K. Harris, A.and Naik. Autonomous command and control for earth-observing satellites using deep reinforcement learning. In *2023 IEEE Aerospace Conference*, pages 1–11, 2023.
- [45] K. Sundar, S.and Ntaimo L.and Darbha S. Qin, J.and Rathinam, and C. Valicka. Algorithms for a satellite constellation scheduling problem. In *2016 IEEE International Conference on Automation Science and Engineering (CASE)*, pages 373–378, 2016.
- [46] A. Globus, J. Crawford, J. Lohn, and A. Pryor. A comparison of techniques for scheduling earth observing satellites. In *Proceedings of the Nineteenth National Conference on Artificial Intelligence*, 2004.
- [47] pulp documentation team. Optimization with pulp. <https://coin-or.github.io/pulp/>, 2009. Accessed: 23 July 2023.
- [48] IBM Corporation. User’s manual for cplex. <https://www.ibm.com/docs/en/icos/12.8.0.0?topic=cplex-users-manual>, 2017. Accessed: 23 July 2023.
- [49] Forrest,J. et al. Coin-or linear programming solver. <https://github.com/coin-or/Clp>, 2023. Accessed: 23 July 2023.
- [50] Spire Global, Inc. Ororatech selects spire global to provide eight satellites for wildfire monitoring constellation. <https://ir.spire.com/news-events/press-releases/detail/173/ororatech-selects-spire-global-to-provide-eight-satellites>, 2023. Accessed: 25 July 2023.